Journal of Marine Science and Technology

Volume 26 | Issue 1 Article 4

FREE VIBRATION ANALYSIS OF A NONLINEARLY TAPERED BEAM CARRYING ARBITRARY CONCENTRATED ELEMENTS BY USING THE CONTINUOUS-MASS TRANSFER MATRIX METHOD

Ching-An Huang
Department of Systems and Naval Mechatronic Engineering, National Cheng-Kung University, Tainan, Taiwan, R.O.C., p18991056@gmail.com

Jong-Shyong Wu
Department of Systems and Naval Mechatronic Engineering, National Cheng-Kung University, Tainan, Taiwan, R.O.C

Heiu-Jou Shaw
Department of Systems and Naval Mechatronic Engineering, National Cheng-Kung University, Tainan, Taiwan, R.O.C.

Recommended Citation

Huang, Ching-An; Wu, Jong-Shyong; and Shaw, Heiu-Jou (2018) "FREE VIBRATION ANALYSIS OF A NONLINEARLY TAPERED BEAM CARRYING ARBITRARY CONCENTRATED ELEMENTS BY USING THE CONTINUOUS-MASS TRANSFER MATRIX METHOD," *Journal of Marine Science and Technology*: Vol. 26: Iss. 1, Article 4.
DOI: 10.6119/JMST.2018.02_(1).0006
Available at: https://jmstt.ntou.edu.tw/journal/vol26/iss1/4

Journal of Marine Science and Technology, Vol. 26, No. 1, pp. 28-49 (2018)
DOI: 10.6119/JMST.2018.02_(1).0006

FREE VIBRATION ANALYSIS OF A NONLINEARLY TAPERED BEAM CARRYING ARBITRARY CONCENTRATED ELEMENTS BY USING THE CONTINUOUS-MASS TRANSFER MATRIX METHOD

Ching-An Huang, Jong-Shyong Wu, and Heiu-Jou Shaw

Key words: exact solution, nonlinearly tapered beam, concentrated elements, non-classical boundary conditions.

ABSTRACT

Although the *exact* solutions for the free vibration problems regarding most of the *non-uniform* beams are not yet obtainable, this is not true for the special case when the equation of motion of a *non-uniform* beam can be transformed into that of an *equivalent* uniform beam. The *nonlinearly* tapered beam studied in this paper is a single-tapered beam with constant depth h_0 and varying width $b(x)$ along its length in the form $b(x) = b_0[1+\alpha(x/L)]^4$, where b_0 is the minimum width, α is the taper constant, x is the axial coordinate and L is the total beam length. For the case of no concentrated elements (CEs) attaching to it, the exact solution for its lowest several natural frequencies and the associated mode shapes has been appeared in the existing literature, however, the *exact* solution for the free vibrations of the last tapered beam carrying various CEs in various boundary conditions (BCs) is not found yet due to complexity of the problem. This is the reason why this paper aims at studying the title problem by using the continuous-mass transfer matrix method (CTMM). It is different from the general *uniform* (or *multi-step*) beam carrying various CEs in that the nonlinearly *tapered* beam itself as well as the attached *translational* and *rotational* CEs must all be transformed into the *equivalent* ones in the derivations. In addition to the solution accuracy, one of the salient merits of the proposed method is that the order of the characteristic-equation matrix keeps constant (4 × 4) and does not increase with the total number of the CEs or the beam segments such as in the conventional finite element method (FEM), so that it needs less than 0.2% of the CPU time required by the FEM to achieve the exact solutions. The CEs on the *nonlinearly* tapered beam include lumped masses (with eccentricities and rotary inertias), translational springs and rotational springs. The formulation of this paper is available for various *classical* or *non-classical* BCs. In addition to comparing with the existing available data, most of the numerical results obtained from the proposed method are also compared with those of the FEM and good agreement is achieved.

Paper submitted 09/17/16; revised 01/13/17; accepted 08/03/17. Author for correspondence: Ching-An Huang (e-mail: p18991056@gmail.com).
Department of Systems and Naval Mechatronic Engineering, National Cheng-Kung University, Tainan, Taiwan, R.O.C.

Fig. 1. The vortex wind generator developed by Vortex Bladeless (2015).

I. INTRODUCTION

According to the report of Owano (2015), the Vortex Bladeless company has developed a bladeless wind turbine as shown in Fig. 1. Instead of turning the parts, the bladeless turbine *oscillates* to produce movement and displacement. The system is based on the same principles as an alternator - electromagnetic induction. The inventors multiply the movement and speed magnetically (without any gear assemblies or ball bearings), and transform the "mechanical energy" of the structure into electricity. From Fig. 1. one sees that the "vortex wind generator" is different from the conventional wind turbine in that it has no spinning blades and looks like nothing except for a nonlinearly tapered beam oscillating in the wind. It is evident that the "mechanical energy" of an oscillating beam carrying concentrated elements (CEs), such as the point masses with eccentricities and rotary inertias, is dependent on its natural frequencies and mode shapes, and the latter are dependent on the *magnitudes* and *distributions* of the attached CEs.

The title problem of this paper is useful for the development of the last *vortex wind turbine*. Furthermore, the free vibration characteristics of an "oscillating beam" are also dependent on its boundary conditions (BCs), and for a clamped-free (C-F) beam such as the vortex wind turbine shown in Fig. 1, the "nonclassical" (or non-zero) BCs presented in this paper can provide its lower end (at $i = 1$) with *variable* translational stiffness ($0 \le 0 \le k_{r,1} \le \infty$) and rotational stiffness ($0 \le k_{r,1} \le \infty$) to achieve *various* natural frequencies and associated mode shapes. Thus, in addition to the theory regarding the CEs, the theory regarding the non-classical (or non-zero) BCs presented in this paper will also be useful for the development of the vortex wind turbine.

Comparing with the *uniform* beams, the literature concerning the *exact* solutions for the free vibrations of the *non-uniform* beams is relatively rare, particularly for those of the "loaded" *non-uniform* beams with various concentrated elements (CEs) attached. Among the various *non-uniform* beams, the *linearly tapered* beams and the *stepped* beams are most popular. Since the title of this paper is relating to the *nonlinearly* tapered beams, only a little literature regarding the *linearly tapered* beams and the *stepped* beams is mentioned here. For the (bare or loaded) *linearly tapered* beams, either with exact or approximate solutions, the works of Cranch and Adler (1956), Naguleswaran (1992), Craver and Jampala (1993), Auciello (1996), Auciello and Maurizi (1997), Wu and Chen (2003), and Wu and Chiang (2004) are relevant; on the other hand, for the *stepped* beams, the works of Tong and Tabarrok (1995c), Rosa et al. (1995b), Naguleswaran (2002), Lin (2006) and Mao (2011) are related. The literature regarding the "loaded" *uniform* beams (carrying various CEs) presented by Liu and Huang (1988), Wu and Chou (1999), and Lin (2008) is also useful for the free vibration analyses of the "loaded" *non-uniform* beams.

For the *variable section* beams, Cranch and Adler (1956) have presented the *exact* solutions for free vibrations of seven *bare* beams by using the Bessel functions or power series, but most of them are for *linearly* tapered beams with exponents $n = 1$, 2 and 3/2, and only two solutions are for the *nonlinearly* tapered beams. Instead of the foregoing Bessel-function solutions, Abrate (1995a) presented the *exact* solution for the free vibration of a *nonlinearly* tapered *bare* beam by using the conventional uniform-beam theory, where the equation of motion for the *nonlinearly* tapered beam must be transformed into that for the *equivalent* uniform beam, first. Based on the last *exact* solution given by Abrate (1995a), Wu and Hsieh (2000) determined the *approximate* natual frequencies and mode shapes of the *nonlinearly* tapered *loaded* beam (carrying multiple point masses) by using the analytical-and-numerical-combined method (ANCM). In addition, Banerjee and Williams (1985) have derived the exact Bernoulli-Euler dynamic stiffness matrix for a range of tapered *bare* beams, however, their stiffness matrix for various tapered beam elements are seldom used, because, in practice, each non-uniform beam is replaced by an *equivalent* stepped beam composed of a number of *uniform* beam segments for the conventional finite element analysis. Recently, Torabi et al. (2013) perform the free vibration analysis of a nonlinerly tapered cantilever Timoshenko *loaded* beam (carrying multiple concentrated masses) by using the differential quadrature element method (DQEM), but it is similarly to the conventional FEM in that their results are the *approximate* solutions instead of the *exact* ones.

From the foregoing literature reviews it is seen that the *exact* solution for the free vibrations of a *nonlinearly* tapered "loaded" beam (carrying various CEs) is not yet obtained, and this is the reason why the title problem is studied here. First of all, the equation of motion for the entire *nonlinearly* tapered *bare* beam is transformed into that for the *equivalent uniform* bare beam, then the latter equivalent *uniform* bare beam is subdivided into several beam segments according to the positions of all sets of CEs, and, in succession, the displacement function for each equivalent uniform beam segment is derived. Next, considering the effects of the ith set of CEs (consisting of a lumped mass m_i with eccentricity e_i and rotary inertia J_i, a translational spring with stiffness $k_{t,i}$ and a rotational spring with stiffness $k_{r,i}$, for $i = 1$ to $n + 1$), the compatibility equations for the displacements and slopes as well as the equilibrium equations for the shear forces and bending moments at each intermediate attaching node i (for the ith set of CEs) are derived, and, based on the theory of continuous-mass transfer matrix method (CTMM) presented by Bapat and Bapat (1987) and Wu and Chen (2008), the transfer matrix for the two adjacent beam segments joined at node i is obtained. Finally, the combination of all transfer matrices for all the intermediate attaching nodes along the beam length and those for the two nodes at the both ends of the entire tapered beam produces a characteristic equation of the form $[W]\{\eta\}_1 = 0$. Now, from the frequency equation $|W| = 0$ one may determine the rth natural frequency of the entire nonlinearly tapered *loaded* beam, ω_r ($r = 1, 2, 3, \ldots$), and corresponding to each frequency ω_r one may obtain the associated vector for the constants of the first beam segment, $\{\eta\}_1 = [A_1, B_1, C_1, D_1]^T$, from the equation $[W]\{\eta\}_1 = 0$, and, in turn, those of the other beam segments, $\{\eta\}_1 = [A_1, B_1, C_1, D_1]^T$ (with $i = 2$ to n). It is obvious that the substitution of all constants, A_i, B_i, C_i and D_i ($i = 1$ to n), into the displacement functions for all the associated beam segments will determine the rth mode shape of the entire nonlineraly tapered *loaded* beam, $Y_r(x) = \sum_{i=1}^{n} V_{r,i}(x) / \varphi_i(x)$, where $V_{r,i}(x)$ and $\varphi_i(x)$ are the rth mode shape and transformation function for the ith equivalent uniform beam segment, respectively.

To show the availability of the presented approach (CTMM), several numerical examples are studied, and it is found that all results of the CTMM are very close to those of the existing literature or the FEM. Because the order of the characteristic-equation matrix derived from the CTMM keeps constant (4×4) instead of increasing with the total number of CEs or beam segments, the computer memory and the CPU time required by the CTMM are much less than those required by the FEM for achieving the same accuracy.

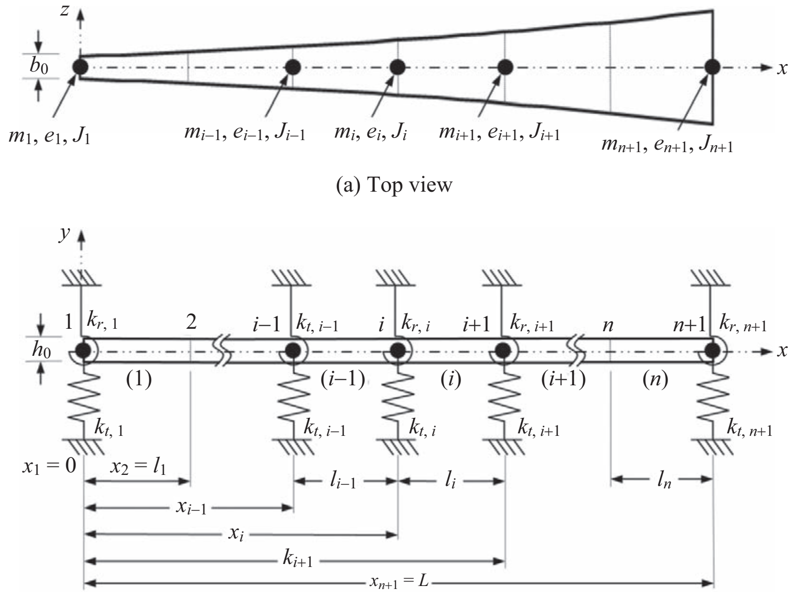

(a) Top view

(b) Front view

Fig. 2. A *nonlinearly* tapered free-free (F-F) beam with taper constant $\alpha = 0.5$ and carrying n+1 identical sets of CEs, with each set of CEs consisting of a lumped mass m_i (with eccentricity e_i and rotary inertia J_i), a translational spring with stiffness $k_{t,i}$ and a rotational spring with stiffness $k_{r,i}$, at each node i (i = 1 to n+1).

II. EQUATION OF MOTION AND DISPLACEMENT FUNCTION

The sketch for the nonlinearly tapered free–free (F-F) beam for the present study is shown in Fig. 2. It is composed of n nonlinearly tapered beam segments (denoted by (1), (2), …, (i–1), (i), (i+1), …, (n)) and n+1 nodes (denoted by 1, 2, …, i–1, i, i+1, …, n+1). Furthermore, each node i is attached by a set of concentrated elements (CEs) consisting of a lumped mass m_i (with eccentricity e_i and rotary inertia J_i), a translational spring with stiffness $k_{t,i}$ and a rotational spring with stiffness $k_{r,i}$. For the free transverse vibration of the ith beam segment (cf. Fig. 2), its equation of motion is given by (Meirovitch, 1967)

$$\frac{\partial^2}{\partial x^2}\left[E_i I_i(x)\frac{\partial^2 y_i(x,t)}{\partial x^2}\right] + \rho_i A_i(x)\frac{\partial^2 y_i(x,t)}{\partial t^2} = 0 \quad (\text{for } x_i \le x \le x_{i+1}) \tag{1}$$

where E_i, ρ_i and $A_i(x)$ are the Young's modulus, mass density and cross-sectional area of the ith beam segment, respectively, and $I_i(x)$ is the moment of inertia of the cross-sectional area $A_i(x)$ located at the axial coordinate x.

According to Abrate (1995a) and Wu and Hsieh (2000), if $I_i(x)$ and $A_i(x)$ take the following forms

$$I_i(x) = I_0\varphi_i^2(x) = I_0\left[1+\alpha\left(\frac{x}{L}\right)\right]^4 = I_0(1+\bar{\alpha}x)^4 \quad (\text{for } x_i \le x \le x_{i+1}) \tag{2}$$

$$A_i(x) = A_0\varphi_i^2(x) = A_0\left[1+\alpha\left(\frac{x}{L}\right)\right]^4 = A_0(1+\bar{\alpha}x)^4 \quad (\text{for } x_i \le x \le x_{i+1}) \tag{3}$$

with

$$\varphi_i(x) = (1+\bar{\alpha}x)^2, \quad \bar{\alpha} = \alpha/L \tag{4a, b}$$

then Eq. (1) can be transformed into

$$E_i I_0 \frac{\partial^4[\varphi_i(x)y_i(x,t)]}{\partial x^4} + \rho_i A_0 \frac{\partial^2[\varphi_i(x)y_i(x,t)]}{\partial t^2} = 0 \quad (\text{for } x_i \le x \le x_{i+1}) \tag{5}$$

In the above equations, A_0 is the smallest cross-sectional area of the entire beam at $x = 0$, I_0 is the corresponding smallest moment of inertia of A_0, L is the total beam length, α is a *positive* taper constant to represent the variation of the entire beam along the beam length.

From Wu and Hsieh (2000), it is seen that, in addition to the *positive* taper constant α, Eq. (4) can also accommodate the *negative* taper constant if it is replaced by

$$\varphi_i(x) = (\varepsilon+\bar{\alpha}x)^2 \quad (\text{for } x_i \le x \le x_{i+1}) \tag{6}$$

with

$$\varepsilon = 1.0, \text{ if } \bar{\alpha} = \alpha/L \ge 0 \tag{7a}$$

$$\varepsilon = 1.0 + |\bar{\alpha}| L \text{, if } \bar{\alpha} = \alpha/L < 0 \quad (7b)$$

For convenience, Eq. (5) is rewritten below

$$E_i I_0 \frac{\partial^4 v_i(x,t)}{\partial x^4} + \rho_i A_0 \frac{\partial^2 v_i(x,t)}{\partial t^2} = 0 \text{ (for } x_i \le x \le x_{i+1}) \quad (8)$$

where

$$v_i(x,t) = \varphi_i(x) y_i(x,t) \quad (9)$$

For free vibrations, one has

$$v_i(x,t) = V_i(x) e^{j\omega t}, \ y_i(x,t) = Y_i(x) e^{j\omega t} \quad (10a, b)$$

where $V_i(x)$ and $Y_i(x)$ are the amplitude functions of $v_i(x,t)$ and $y_i(x,t)$, respectively, ω is the natural frequency of the entire nonlinearly tapered beam, t is time and $j = \sqrt{-1}$.

Substituting Eqs. (10a, b) into Eqs. (8) and (9), one obtains

$$V_i''''(x) - \beta_i^4 V_i(x) = 0 \text{ (for } x_i \le x \le x_{i+1}) \quad (11)$$

$$V_i(x) = \varphi_i(x) Y_i(x) \text{ (for } x_i \le x \le x_{i+1}) \quad (12)$$

with

$$\beta_i^4 = \omega^2 \rho_i A_0 / (E_i I_0) \quad (13)$$

where the primes denote differentiations with respect to the axial coordinate x.

The solution of Eq. (11) takes the form (Meirovitch, 1967)

$$\begin{aligned} V_i(x) = A_i(\cos\beta_i x + \cosh\beta_i x) + B_i(\cos\beta_i x - \cosh\beta_i x) \\ + C_i(\sin\beta_i x + \sinh\beta_i x) \\ + D_i(\sin\beta_i x - \sinh\beta_i x) \end{aligned} \quad (14)$$

where A_i, B_i, C_i and D_i are the constants for the ith equivalent uniform beam segment.

From Eqs. (6) and (12), one obtains

$$V_i'(x) = \varphi_i'(x) Y_i(x) + \varphi_i(x) Y_i'(x) \quad (15a)$$

$$V_i''(x) = \varphi_i''(x) Y_i(x) + 2\varphi_i'(x) Y_i'(x) + \varphi_i(x) Y_i''(x) \quad (15b)$$

$$\begin{aligned} V_i'''(x) = \varphi_i'''(x) Y_i(x) + 3\varphi_i''(x) Y_i'(x) \\ + 3\varphi_i'(x) Y_i''(x) + \varphi_i(x) Y_i'''(x) \end{aligned} \quad (15c)$$

$$\varphi_i'(x) = 2\bar{\alpha}(\varepsilon + \bar{\alpha} x), \ \varphi_i''(x) = 2\bar{\alpha}^2, \ \varphi_i'''(x) = 0 \quad (16a\text{-}c)$$

III. TRANSFER MATRIX FOR AN INTERMEDIATE ATTACHING NODE *i*

For the nonlinearly tapered beam shown in Fig. 2, the continuity of displacements and slopes, as well as the equilibrium of shear forces and bending moments for the two adjacent beam segments, (i–1) and (i), joined at the intermediate attaching node i for the ith set of CEs (located at $x = x_i$) require that

$$V_{i-1}(x_i) = V_i(x_i) \quad (17a)$$

$$V_{i-1}'(x_i) = V_i'(x_i) \quad (17b)$$

$$\begin{aligned} E_{i-1} I_0 V_{i-1}''(x_i) = E_i I_0 V_i''(x_i) + F_{e,i} \bar{Y}_i(x_i) \\ - K_{r,i} \bar{Y}_i'(x_i) \end{aligned} \quad (17c)$$

$$E_{i-1} I_0 V_{i-1}'''(x_i) = E_i I_0 V_i'''(x_i) + K_{t,i} \bar{Y}_i(x_i) - F_{e,i} \bar{Y}_i'(x_i) \quad (17d)$$

where $\bar{Y}_i(x_i)$ is the "transformed" displacement function associated with the *translational* CEs (such as mi and $k_{t,i}$) located at $x = x_i$ given by Eq. (A.6) (in the **Appendix A** at the end of this paper)

$$\bar{Y}_i(x_i) = V_i(x_i) / \varphi^2(x_i) \quad (18a)$$

and $\bar{Y}_i'(x_i)$ is the derivative of $\bar{Y}_i(x_i)$ associated with *rotational* CEs (such as J_i and $k_{r,i}$) as one may see from Eq. (A.7). Furthermore, the expressions for the parameters $k_{t,i}$, $k_{r,i}$ and $F_{e,i}$ are respectively given by Wu and Chen (2008)

$$K_{t,i} = k_{t,i} - m_i\omega^2, \ K_{r,i} = k_{r,i} - (J_i + m_i e_i^2)\omega^2, \ F_{e,i} = m_i e_i \omega^2 \quad (18b\text{-}d)$$

In the above equations, $k_{t,i}$ and $k_{r,i}$ denote the *translational* and *rotational* effective stiffnesses due to the associated CEs attached to node i [such as $k_{t,i}$, $k_{r,i}$ and m_i (with e_i and J_i)], respectively, and $F_{e,i}$ denotes the centrifugal force due to eccentricity e_i of the lumped mass m_i.

The substitution of the function $\bar{Y}_i(x_i)$ given by Eq. (18a) into Eqs. (17c, d) produces

$$\begin{aligned} E_{i-1} I_0 V_{i-1}''(x_i) = E_i I_0 V_i''(x_i) + \frac{F_{e,i}}{\varphi_i^2} V(x_i) + \frac{K_{r,i}}{\varphi_i^2} V_i'(x_i) \\ - \frac{2\varphi_i \varphi_i' K_{r,i}}{\varphi_i^4} V_i(x_i) \end{aligned} \quad (17c)'$$

$$\begin{aligned} E_{i-1} I_0 V_{i-1}'''(x_i) = E_i I_0 V_i'''(x_i) + \frac{K_{t,i}}{\varphi_i^2} V_i(x_i) - \frac{F_{e,i}}{\varphi_i^2} V_i'(x_i) \\ + \frac{2\varphi\varphi' F_{e,i}}{\varphi_i^4} V_i(x_i) \end{aligned} \quad (17d)'$$

In the last two equations, we set $\varphi_i(x_i) = \varphi_i$, for simplicity.

Introducing the function $V(x)$ given by Eq. (14) into Eqs. (17a, b) and (17c, d)', respectively, one obtains

$$\begin{aligned} &A_{i-1}(\cos\theta_{i-1} + \cosh\theta_{i-1}) + B_{i-1}(\cos\theta_{i-1} - \cosh\theta_{i-1}) \\ &\quad + C_{i-1}(\sin\theta_{i-1} + \sinh\theta_{i-1}) \\ &\quad + D_{i-1}(\sin\theta_{i-1} - \sinh\theta_{i-1}) \\ &= A_i(\cos\theta_i + \cosh\theta_i) + B_i(\cos\theta_i - \cosh\theta_i) \\ &\quad + C_i(\sin\theta_i + \sinh\theta_i) \\ &\quad + D_i(\sin\theta_i - \sinh\theta_i) \end{aligned} \tag{19a}$$

$$\begin{aligned} &A_{i-1}(-\sin\theta_{i-1} + \sinh\theta_{i-1}) + B_{i-1}(-\sin\theta_{i-1} - \sinh\theta_{i-1}) \\ &\quad + C_{i-1}(\cos\theta_{i-1} + \cosh\theta_{i-1}) \\ &\quad + D_{i-1}(\cos\theta_{i-1} - \cosh\theta_{i-1}) \\ &= \beta_i^*[A_i(-\sin\theta_i + \sinh\theta_i) + B_i(-\sin\theta_i - \sinh\theta_i) \\ &\quad + C_i(\cos\theta_i + \cosh\theta_i) \\ &\quad + D_i(\cos\theta_i - \cosh\theta_i)] \end{aligned} \tag{19b}$$

$$\begin{aligned} &A_{i-1}(-\cos\theta_{i-1} + \cosh\theta_{i-1}) + B_i(-\cos\theta_{i-1} - \cosh\theta_{i-1}) \\ &\quad + C_i(-\sin\theta_{i-1} + \sinh\theta_{i-1}) \\ &\quad + D_i(-\sin\theta_{i-1} - \sinh\theta_{i-1}) \\ &= A_iN_i + B_iP_i + C_iR_i + D_iQ_i \end{aligned} \tag{19c}$$

$$\begin{aligned} &A_{i-1}(\sin\theta_{i-1} + \sinh\theta_{i-1}) + B_{i-1}(\sin\theta_{i-1} - \sinh\theta_{i-1}) \\ &\quad + C_{i-1}(-\cos\theta_{i-1} + \cosh\theta_{i-1}) \\ &\quad + D_{i-1}(-\cos\theta_{i-1} - \cosh\theta_{i-1}) \\ &= A_i\bar{N}_i + B_i\bar{P}_i + C_i\bar{R}_i + D_i\bar{Q}_i \end{aligned} \tag{19d}$$

where

$$N_i = [-\tilde{\delta}_i\cos\theta_i + \hat{\delta}_i\cosh\theta_i + \tilde{\kappa}_i(-\sin\theta_i + \sinh\theta_i)]\big/E_{i-1}I_0\beta_{i-1}^2 \tag{20a}$$

$$P_i = [-\tilde{\delta}_i\cos\theta_i - \hat{\delta}_i\cosh\theta_i + \tilde{\kappa}_i(-\sin\theta_i - \sinh\theta_i)]\big/E_{i-1}I_0\beta_{i-1}^2 \tag{20b}$$

$$R_i = [-\tilde{\delta}_i\sin\theta_i + \hat{\delta}_i\sinh\theta_i + \tilde{\kappa}_i(\cos\theta_i + \cosh\theta_i)]\big/E_{i-1}I_0\beta_{i-1}^2 \tag{20c}$$

$$Q_i = [-\tilde{\delta}_i\sin\theta_i - \hat{\delta}_i\sinh\theta_i + \tilde{\kappa}_i(\cos\theta_i - \cosh\theta_i)]\big/E_{i-1}I_0\beta_{i-1}^2 \tag{20d}$$

$$\bar{N}_i = [\tilde{\lambda}_i\sin\theta_i + \hat{\lambda}_i\sinh\theta_i + \hat{\kappa}_i(\cos\theta_i + \cosh\theta_i)]\big/E_{i-1}I_0\beta_{i-1}^3 \tag{21a}$$

$$\bar{P}_i = [\tilde{\lambda}_i\sin\theta_i - \hat{\lambda}_i\sinh\theta_i + \hat{\kappa}_i(\cos\theta_i - \cosh\theta_i)]\big/E_{i-1}I_0\beta_{i-1}^3 \tag{21b}$$

$$\bar{R}_i = [-\tilde{\lambda}_i\cos\theta_i + \hat{\lambda}_i\cosh\theta_i + \hat{\kappa}_i(\sin\theta_i + \sinh\theta_i)]\big/E_{i-1}I_0\beta_{i-1}^3 \tag{21c}$$

$$\bar{Q}_i = [-\tilde{\lambda}_i\cos\theta_i - \hat{\lambda}_i\cosh\theta_i + \hat{\kappa}_i(\sin\theta_i - \sinh\theta_i)]\big/E_{i-1}I_0\beta_{i-1}^3 \tag{21d}$$

$$\tilde{\delta}_i = E_iI_0\beta_i^2 - \left(\frac{F_{e,i}}{\varphi_i^2} - \frac{2\varphi_i\varphi_i'K_{r,i}}{\varphi_i^4}\right), \quad \hat{\delta}_i = E_iI_0\beta_i^2 + \left(\frac{F_{e,i}}{\varphi_i^2} - \frac{2\varphi_i\varphi_i'K_{r,i}}{\varphi_i^4}\right), \tag{22a, b}$$

$$\tilde{\lambda}_i = E_iI_0\beta_i^3 + \frac{\beta_iF_{e,i}}{\varphi_i^2}, \quad \hat{\lambda}_i = E_iI_0\beta_i^3 - \frac{\beta_iF_{e,i}}{\varphi_i^2}, \tag{23a, b}$$

$$\tilde{\kappa}_i = \frac{\beta_iK_{r,i}}{\varphi_i^2}, \quad \hat{\kappa}_i = \frac{K_{t,i}}{\varphi_i^2} + \frac{2\varphi\varphi'F_{e,i}}{\varphi_i^4} \tag{24a, b}$$

$$\theta_{i-1} = \beta_{i-1}x_i, \quad \theta_i = \beta_ix_i, \quad \beta_i^* = \beta_i/\beta_{i-1} \tag{25a-c}$$

Writing Eqs. (19a-d) in matrix form, one has

$$[G]_{i-1}\{\eta\}_{i-1} = [H]_i\{\eta\}_i \tag{26}$$

where

$$\{\eta\}_i = [A_i \quad B_i \quad C_i \quad D_i]^T, \quad \{\eta\}_{i-1} = [A_{i-1} \quad B_{i-1} \quad C_{i-1} \quad D_{i-1}]^T \tag{27a, b}$$

$$[G]_{i-1} = \begin{bmatrix} \cos\theta_{i-1} + \cosh\theta_{i-1} & \cos\theta_{i-1} - \cosh\theta_{i-1} & \sin\theta_{i-1} + \sinh\theta_{i-1} & \sin\theta_{i-1} - \sinh\theta_{i-1} \\ -\sin\theta_{i-1} + \sinh\theta_{i-1} & -\sin\theta_{i-1} - \sinh\theta_{i-1} & \cos\theta_{i-1} + \cosh\theta_{i-1} & \cos\theta_{i-1} - \cosh\theta_{i-1} \\ -\cos\theta_{i-1} + \cosh\theta_{i-1} & -\cos\theta_{i-1} - \cosh\theta_{i-1} & -\sin\theta_{i-1} + \sinh\theta_{i-1} & -\sin\theta_{i-1} - \sinh\theta_{i-1} \\ \sin\theta_{i-1} + \sinh\theta_{i-1} & \sin\theta_{i-1} - \sinh\theta_{i-1} & -\cos\theta_{i-1} + \cosh\theta_{i-1} & -\cos\theta_{i-1} - \cosh\theta_{i-1} \end{bmatrix} \tag{28}$$

$$[H]_i = \begin{bmatrix} \cos\theta_i + \cosh\theta_i & \cos\theta_i - \cosh\theta_i & \sin\theta_i + \sinh\theta_i & \sin\theta_i - \sinh\theta_i \\ \beta_i^*(-\sin\theta_i + \sinh\theta_i) & \beta_i^*(-\sin\theta_i - \sinh\theta_i) & \beta_i^*(\cos\theta_i + \cosh\theta_i) & \beta_i^*(\cos\theta_i - \cosh\theta_i) \\ N_i & P_i & R_i & Q_i \\ \bar{N}_i & \bar{P}_i & \bar{R}_i & \bar{Q}_i \end{bmatrix} \tag{29}$$

From Eq. (26) one obtains

$$\{\eta\}_i = [H]_i^{-1}[G]_{i-1}\{\eta\}_{i-1} = [T]_{i-1}\{\eta\}_{i-1} \tag{30}$$

where

$$[T]_{i-1} = [H]_i^{-1}[G]_{i-1} \tag{31}$$

which represents the transfer matrix between the constants for beam segment (i), $\{\eta\}_i$, and those for beam segment (i-1), $\{\eta\}_{i-1}$, joined at the intermediate attaching node i.

From Eq. (30), one has

$$\begin{aligned} \{\eta\}_n &= [T]_{n-1}\{\eta\}_{n-1} = [T]_{n-1}[T]_{n-2}\{\eta\}_{n-2} \\ &= \cdots = [T]_{n-1}[T]_{n-2}\cdots[T]_2[T]_1\{\eta\}_1 = [T]\{\eta\}_1 \end{aligned} \tag{32}$$

where

$$[T]=[T]_{n-1}[T]_{n-2}\cdots[T]_2[T]_1=\begin{bmatrix} T_{11} & T_{12} & T_{13} & T_{14} \\ T_{21} & T_{22} & T_{23} & T_{24} \\ T_{31} & T_{32} & T_{33} & T_{34} \\ T_{41} & T_{42} & T_{43} & T_{44} \end{bmatrix} \quad (33)$$

IV. EQUATIONS REGARDING *NON-CLASSICAL* BOUNDARY CONDITIONS

For convenience, the BCs of a beam with its *ends* attached by various CEs as shown in Fig. 2 are called the *non-classical* BCs. On the contrary, for a beam without any CEs attached to its *ends*, its BCs are called the *classical* BCs. The equations regarding the *non-classical* BCs of a nonlinearly tapered beam are derived in this section, and those regarding the *classical* BCs are derived in the **Appendix B** at the end of this paper.

1. The BCs for a Free-Free (F-F) Beam

For a *free-free* (F-F) beam, the BCs at its *left* end (i.e., at left end of the 1st beam segment) are given by

$$E_1 I_0[V_1''(0)+6\lambda^2 V_1(0)-4\lambda V_1'(0)] + F_{e,1}\bar{Y}_1(0)-K_{r,1}\bar{Y}_1'(0)=0 \quad (34a)$$

$$E_1 I_0[V_1'''(0)+12\lambda^3 V_1(0)-6\lambda^2 V_1'(0)] + K_{t,1}\bar{Y}_1(0)-F_{e,1}\bar{Y}_1'(0)=0 \quad (34b)$$

where

$$\lambda=\bar{\alpha}/\varepsilon \quad (34c)$$

In Eq. (34a) or (34b), the first term is the BC for the *left* free end without any CEs as shown in Eq. (A.9a) or (A.9b) in the **Appendix B** at the end of this paper, while the 2nd and 3rd terms are the bending moments or shear forces due to the CEs as one may see from Eqs. (17c, d).

The substitution of the function $Y_i(x_i)$, with i = 1, given by Eq. (18a) into Eqs. (34a, b) yields

$$E_1 I_0[V_1''(0)+6\lambda^2 V_1(0)-4\lambda V_1'(0)] + \frac{F_{e,1}}{\varphi_1^2}V_1(0)+\frac{K_{r,1}}{\varphi_1^2}V_1'(0) - \frac{2\varphi_1\varphi_1' K_{r,1}}{\varphi_1^4}V_1(0)=0 \quad (35a)$$

$$E_1 I_0[V_1'''(0)+12\lambda^3 V_1(0)-6\lambda^2 V_1'(0)] + \frac{K_{t,1}}{\varphi_1^2}V_1(0)-\frac{F_{e,1}}{\varphi_1^2}V_1'(0) + \frac{2\varphi_1\varphi_1' F_{e,1}}{\varphi_1^4}V_1(0)=0 \quad (35b)$$

In Eqs. (35a,b), we set $\varphi_1(0)=\varphi_1$, for simplicity.
Substituting Eq. (14) into Eqs. (35a, b), one obtains

$$S_{11}A_1+S_{12}B_1+S_{13}C_1+S_{14}D_1=0 \quad (36a)$$

$$S_{21}A_1+S_{22}B_1+S_{23}C_1+S_{24}D_1=0 \quad (36b)$$

where

$$S_{11}=12E_1 I_0\lambda^2+2F_{e,1}/\varphi_1^2-4\varphi_1\varphi_1' K_{r,1}/\varphi_1^4\ ,\ S_{12}=-2E_1 I_0\beta_1^2 \quad (37a,\ b)$$

$$S_{13}=-8E_1 I_0\lambda\beta_1+2\beta_1 K_{r,1}/\varphi_1^2\ ,\ S_{14}=0 \quad (37c,\ d)$$

$$S_{21}=24E_1 I_0\lambda^3+2K_{t,1}/\varphi_1^2+4\varphi_1\varphi_1' F_{e,1}/\varphi_1^4\ ,\ S_{22}=0 \quad (38a,\ b)$$

$$S_{23}=-12E_1 I_0\lambda^2\beta_1-2\beta_1 F_{e,1}/\varphi_1^2\ ,\ S_{24}=-2E_1 I_0\beta_i^3 \quad (38c,\ d)$$

Similarly, the BCs at right end of the entire beam (i.e., at right end of the nth beam segment) are given by

$$E_n I_0[V_n''(L)+6\mu^2 V_n(L)-4\mu V_n'(L)] - F_{e,n+1}\bar{Y}_n(L)+K_{r,n+1}\bar{Y}_n'(L)=0 \quad (39a)$$

$$E_n I_0[V_n'''(L)+12\mu^3 V_n(L)-6\mu^2 V_n'(L)] - K_{t,n+1}\bar{Y}_n(L)+F_{e,n+1}\bar{Y}_n'(L)=0 \quad (39b)$$

where

$$\mu=\bar{\alpha}/(\varepsilon+\bar{\alpha}L) \quad (40)$$

In Eq. (39a) or (39b), the first term is the BC for the *right* free end without any CEs as shown in Eq. (A.14a) or (A.14b) in the **Appendix B** at the end of this paper, while the 2nd and 3rd terms are due to the CEs as one may see from Eqs. (17c, d).

Substituting the function $\bar{Y}_i(x_i)$, with i = n, given by Eq. (18a) into Eqs. (39a, b), one obtains

$$E_n I_0[V_n''(L)+6\mu^2 V_n(L)-4\mu V_n'(L)] - \frac{F_{e,n+1}}{\varphi_n^2}V_n(L)-\frac{K_{r,n+1}}{\varphi_n^2}V_n'(L) + \frac{2\varphi_n\varphi_n' K_{r,n+1}}{\varphi_n^4}V_n(L)=0 \quad (41a)$$

$$E_n I_0[V_n'''(L)+12\mu^3 V_n(L)-6\mu^2 V_n'(L)] -\frac{K_{t,n+1}}{\varphi_n^2}V_n(L)+\frac{F_{e,n+1}}{\varphi_n^2}V_n'(L) -\frac{2\varphi_n\varphi_n' F_{e,n+1}}{\varphi_n^4}V_n(L)=0 \quad (41b)$$

For simplicity, we set $\varphi_n(L) = \varphi_n$ in the last two equations. The substitution of Eq. (14) into Eqs. (41a, b) leads to

$$U_{11}A_n + U_{12}B_n + U_{13}C_n + U_{14}D_n = 0 \quad (42a)$$

$$U_{21}A_n + U_{22}B_n + U_{23}C_n + U_{24}D_n = 0 \quad (42b)$$

where

$$U_{11} = E_n I_0 \beta_n^2 \left(-\cos\beta_n L + \cosh\beta_n L\right) + \tilde{\delta}_B \left(\cos\beta_n L + \cosh\beta_n L\right) - \hat{\delta}_B \beta_n \left(-\sin\beta_n L + \sinh\beta_n L\right) \quad (43a)$$

$$U_{12} = E_n I_0 \beta_n^2 \left(-\cos\beta_n L - \cosh\beta_n L\right) + \tilde{\delta}_B \left(\cos\beta_n L - \cosh\beta_n L\right) - \hat{\delta}_B \beta_n \left(-\sin\beta_n L - \sinh\beta_n L\right) \quad (43b)$$

$$U_{13} = E_n I_0 \beta_n^2 \left(-\sin\beta_n L + \sinh\beta_n L\right) + \tilde{\delta}_B \left(\sin\beta_n L + \sinh\beta_n L\right) - \hat{\delta}_B \beta_n \left(\cos\beta_n L + \cosh\beta_n L\right) \quad (43c)$$

$$U_{14} = E_n I_0 \beta_n^2 \left(-\sin\beta_n L - \sinh\beta_n L\right) + \tilde{\delta}_B \left(\sin\beta_n L - \sinh\beta_n L\right) - \hat{\delta}_B \beta_n \left(\cos\beta_n L - \cosh\beta_n L\right) \quad (43d)$$

$$U_{21} = E_n I_0 \beta_n^3 \left(\sin\beta_n L + \sinh\beta_n L\right) + \tilde{\delta}_S \left(\cos\beta_n L + \cosh\beta_n L\right) - \hat{\delta}_S \beta_n \left(-\sin\beta_n L + \sinh\beta_n L\right) \quad (44a)$$

$$U_{22} = E_n I_0 \beta_n^3 \left(\sin\beta_n L - \sinh\beta_n L\right) + \tilde{\delta}_S \left(\cos\beta_n L - \cosh\beta_n L\right) - \hat{\delta}_S \beta_n \left((-\sin\beta_n L - \sinh\beta_n L)\right) \quad (44b)$$

$$U_{23} = E_n I_0 \beta_n^3 \left(-\cos\beta_n L + \cosh\beta_n L\right) + \tilde{\delta}_S \left(\sin\beta_n L + \sinh\beta_n L\right) - \hat{\delta}_S \beta_n \left(\cos\beta_n L + \cosh\beta_n L\right) \quad (44c)$$

$$U_{24} = E_n I_0 \beta_n^3 \left(-\cos\beta_n L - \cosh\beta_n L\right) + \tilde{\delta}_S \left(\sin\beta_n L - \sinh\beta_n L\right) - \hat{\delta}_S \beta_n \left(\cos\beta_n L - \cosh\beta_n L\right) \quad (44d)$$

$$\tilde{\delta}_B = 6E_n I_0 \mu^2 + \frac{F_{e,n+1}}{\varphi_n^2} - \frac{2\varphi_n\varphi_n' K_{r,n+1}}{\varphi_n^4}, \quad \hat{\delta}_B = 4E_n I_0 \mu - \frac{K_{r,n+1}}{\varphi_n^2} \quad (45a, b)$$

$$\tilde{\delta}_S = 12E_n I_0 \mu^3 + \frac{K_{t,n+1}}{\varphi_n^2} + \frac{2\varphi_n\varphi_n' F_{e,n+1}}{\varphi_n^4}, \quad \hat{\delta}_S = 6E_n I_0 \mu^2 + \frac{F_{e,n+1}}{\varphi_n^2} \quad (46a, b)$$

2. The BCs for a P-P Beam

The BCs at the *left* end of the entire P-P beam are given by

$$V_1(0) = 0 \quad (47a)$$

$$E_1 I_0[V_1''(0) + 6\lambda^2 V_1(0) - 4\lambda V_1'(0)] + F_{e,1}\overline{Y}_1(0) - K_{r,1}\overline{Y}_1'(0) = 0 \quad (47b)$$

It is noted that Eq. (47b) is the same as Eq. (34a) for the *left* free end with bending moment to be equal to zero.

Substituting the function $\overline{Y}_i(x_i)$, with i = 1, given by Eq. (18a) into Eq. (47b) and considering the expression $V_1(0) = 0$ given by Eq. (47a), one obtains

$$E_1 I_0[V_1''(0) - 4\lambda V_1'(0)] + \frac{K_{r,1}}{\varphi_1^2}V_1'(0) = 0 \quad (47b)'$$

Substituting Eq. (14) into Eqs. (47a) and (47b)' produces

$$S_{11}A_1 + S_{12}B_1 + S_{13}C_1 + S_{14}D_1 = 0 \quad (48a)$$

$$S_{21}A_1 + S_{22}B_1 + S_{23}C_1 + S_{24}D_1 = 0 \quad (48b)$$

where

$$S_{11} = 2\,,\ S_{12} = S_{13} = S_{14} = 0 \quad (49a\text{-}d)$$

$$S_{21} = 0,$$
$$S_{22} = -2E_1 I_0 \beta_1^2,$$
$$S_{23} = -8E_1 I_0 \lambda \beta_1 + 2\beta_1 K_{r,1} / \varphi_1^2, \tag{50a-d}$$
$$S_{24} = 0$$

Similarly, the BCs at *right* end of the entire P-P beam are given by

$$V_n(L) = 0 \tag{51a}$$

$$E_n I_0 [V_n''(L) + 6\mu^2 V_n(L) - 4\mu V_n'(L)] - F_{e,n+1} \bar{Y}_n(L) + K_{r,n+1} \bar{Y}_n'(L) = 0 \tag{51b}$$

It is evident that Eq. (51b) is the same as Eq. (39a) with bending moment to be equal to zero at the *right* free end.

Introducing the function $\bar{Y}_i(x_i)$, with $i = n$, given by Eq. (18a) into Eq. (51b) and considering the expression $V_n(L) = 0$ given by Eq. (51a), one obtains

$$E_n I_0 [V_n''(L) - 4\mu V_n'(L)] - \frac{K_{r,n+1}}{\varphi_n^2} V_n'(L) = 0 \tag{51b'}$$

Substituting Eq. (14) into Eqs. (51a) and (51b)' produces

$$U_{11} A_n + U_{12} B_n + U_{13} C_n + U_{14} D_n = 0 \tag{52a}$$

$$U_{21} A_n + U_{22} B_n + U_{23} C_n + U_{24} D_n = 0 \tag{52b}$$

where

$$U_{11} = \cos\beta_n L + \cosh\beta_n L,\ U_{12} = \cos\beta_n L - \cosh\beta_n L \tag{53a, b}$$

$$U_{13} = \sin\beta_n L + \sinh\beta_n L,\ U_{14} = \sin\beta_n L - \sinh\beta_n L \tag{53c, d}$$

$$U_{21} = E_n I_0 \beta_n^2 (-\cos\beta_n L + \cosh\beta_n L) - \beta_n (4E_n I_0 \mu + K_{r,n+1} / \varphi_n^2)(-\sin\beta_n L + \sinh\beta_n L) \tag{54a}$$

$$U_{22} = E_n I_0 \beta_n^2 (-\cos\beta_n L - \cosh\beta_n L) - \beta_n (4E_n I_0 \mu + K_{r,n+1} / \varphi_n^2)(-\sin\beta_n L - \sinh\beta_n L) \tag{54b}$$

$$U_{23} = E_n I_0 \beta_n^2 (-\sin\beta_n L + \sinh\beta_n L) - \beta_n (4E_n I_0 \mu + K_{r,n+1} / \varphi_n^2)(\cos\beta_n L + \cosh\beta_n L) \tag{54c}$$

$$U_{24} = E_n I_0 \beta_n^2 (-\sin\beta_n L - \sinh\beta_n L) - \beta_n (4E_n I_0 \mu + K_{r,n+1} / \varphi_n^2)(\cos\beta_n L - \cosh\beta_n L) \tag{54d}$$

3. The BCs for a C-C Beam

Because the displacements and slopes at the both ends of a C-C beam are equal to zero and so are the elastic (or inertial) forces and bending moments induced by the CEs, the associated equations regarding the *non-classical* BCs of a C-C beam are the same as those regarding the *classical* BCs of a C-C beam given by Eqs. (A.26)-(A.33) in the **Appendix B**, and are not repeated here.

It is noted that, for a beam with the BCs of *left* end to be different from the BCs of *right* end (such as the C-F or C-P beam), the equations regarding to its BCs can be obtained from the corresponding ones for the same BCs derived previously (or in the **Appendix B**). For convenience, the CTMM based on the *non-classical* BCs presented in this section is denoted by CTMMn, while that based on the *classical* BCs shown in **Appendix B** is denoted by CTMMc. It is evident that all *classical* BCs shown in **Appendix B** can be obtained from the *non-classical* BCs given in previous **Subsection 4.1** by setting: (i) $m_i = e_i = J_i = k_{t,i} = k_{r,i} = 0$ (with $i = 1$ or $n + 1$) for a *classical* free end, (ii) $k_{t,i}/k_{t,\mathrm{ref}} \geq 10^{15}$ along with $m_i = e_i = J_i = k_{r,i} = 0$ for a *classical* pinned end, and (iii) $k_{t,i}/k_{t,\mathrm{ref}} = k_{r,i}/k_{r,\mathrm{ref}} \geq 10^{15}$ along with $m_i = e_i = J_i = 0$ for a *classical* clamped end, where $k_{r,\mathrm{ref}} = E_1 I_0/L^3$ and $k_{r,\mathrm{ref}} = E_1 I_0/L$ are the *reference* translational and rotational stiffness, respectively. Since all *classical* BCs are equal to zero as one may see from Eqs. (A.8a, b), (A.13a, b), (A.18a, b), (A.22a, b), (A.26a, b) and (A.30a, b), in **Appendix B**, they are also called the *zero* BCs. On the contrary, all *non-classical* BCs shown in **Section 4** are not equal to zero due to the effects of inertial (or restoring) forces or moments of the CEs located at the two ends, they are also called the *non-zero* BCs.

V. DETERMINATION OF NATURAL FREQUENCIES AND MODE SHAPES OF THE ENTIRE BEAM

The natural frequencies and mode shapes of a beam are dependent on its BCs. For convenience, the formulation of this subsection is based on the F-F beam. Writing the two equations for the *right*-end BCs of a F-F beam given by Eqs. (42a, b) in matrix form, one obtains

$$[U]\{\eta\}_n = 0 \tag{55}$$

where

$$[U] = \begin{bmatrix} U_{11} & U_{12} & U_{13} & U_{14} \\ U_{21} & U_{22} & U_{23} & U_{24} \end{bmatrix} \tag{56}$$

Introducing Eq. (32) into Eq. (55), one has

$$[U][T]\{\eta\}_1 = 0 \tag{57}$$

or

$$[Z]\{\eta\}_1 = 0 \tag{58}$$

where

$$[Z]_{2\times 4} = [U]_{2\times 4}[T]_{4\times 4} \tag{59}$$

with

$$Z_{11} = U_{11}T_{11} + U_{12}T_{21} + U_{13}T_{31} + U_{14}T_{41}, \quad Z_{12} = U_{11}T_{12} + U_{12}T_{22} + U_{13}T_{32} + U_{14}T_{42} \tag{60a, b}$$

$$Z_{13} = U_{11}T_{13} + U_{12}T_{23} + U_{13}T_{33} + U_{14}T_{43}, \quad Z_{14} = U_{11}T_{14} + U_{12}T_{24} + U_{13}T_{34} + U_{14}T_{44} \tag{60c, d}$$

$$Z_{21} = U_{21}T_{11} + U_{22}T_{21} + U_{23}T_{31} + U_{24}T_{41}, \quad Z_{22} = U_{21}T_{12} + U_{22}T_{22} + U_{23}T_{32} + U_{24}T_{42} \tag{61a, b}$$

$$Z_{23} = U_{21}T_{13} + U_{22}T_{23} + U_{23}T_{33} + U_{24}T_{43}, \quad Z_{24} = U_{21}T_{14} + U_{22}T_{24} + U_{23}T_{34} + U_{24}T_{44} \tag{61c, d}$$

Combining the other two equations for the *left*-end BCs of the F-F beam given by Eqs. (36a, b) with Eq. (58), one obtains

$$[W]\{\eta\}_1 = 0 \tag{62}$$

where

$$[W] = \begin{bmatrix} S_{11} & S_{12} & S_{13} & S_{14} \\ S_{21} & S_{22} & S_{23} & S_{24} \\ Z_{11} & Z_{12} & Z_{13} & Z_{14} \\ Z_{21} & Z_{22} & Z_{23} & Z_{24} \end{bmatrix} \tag{63}$$

Eq. (62) is the characteristic equation for the nonlinearly tapered *loaded* beam (cf. Fig. 2). Where the order of the coefficient matrix [W] keeps constant (4 × 4) and independent on the total number of beam segments or attached CEs, this is different from the conventional FEM or the other classical analytical methods. Eq. (62) represents a set of simultaneous equations, non-trivial solution for $\{\eta\}_1$ requires that

$$|W| = \begin{vmatrix} S_{11} & S_{12} & S_{13} & S_{14} \\ S_{21} & S_{22} & S_{23} & S_{24} \\ Z_{11} & Z_{12} & Z_{13} & Z_{14} \\ Z_{21} & Z_{22} & Z_{23} & Z_{24} \end{vmatrix} = 0 \tag{64a}$$

or

$$\begin{vmatrix} S_{11} & S_{12} & S_{13} & S_{14} \\ Z_{11} & Z_{12} & Z_{13} & Z_{14} \\ S_{21} & S_{22} & S_{23} & S_{24} \\ Z_{21} & Z_{22} & Z_{23} & Z_{24} \end{vmatrix} = 0 \tag{64b}$$

Eq. (64) is the *frequency* equation, from which one may determine the natural frequencies ω_r (r = 1, 2, 3 …) by using the *conventional* half-interval method (Carnahan et al., 1969) or the *modified* half-interval method (Wu and Chen, 2011), and corresponding to each natural frequency one may obtain the associated constants $\{\eta\}_1 = [A_1 \quad B_1 \quad C_1 \quad D_1]^T$ from Eq. (62). Once the constants for the first beam segment, $\{\eta\}_1$, are determined, those for the other beam segments, $\{\eta\}_i$ (i = 2, 3 …, n), can be obtained from Eq. (30), and substituting the obtained constants for all beam segments, $\{\eta\}_i$ (i = 1, 2, 3 …, n), into Eqs. (14) and (12), one determines the associated mode shape of the entire nonlinearly tapered beam, $Y_r(x) = \sum_{i=1}^{n} V_{r,i}(x)/\varphi_i(x)$.

It is noted that the above formulation is for the F-F beam. For a beam with the other BCs, it is only required to replace the values of $U_{p,q}$ and $S_{p,q}$ (p = 1, 2; q = 1 – 4) appearing in Eqs. (56), (60), (61), (63) and (64) by the corresponding ones associated the specified BCs, such as those given by Eqs. (49), (50), (53) and (54) for the P-P beam.

VI. NUMERICAL RESULTS AND DISCUSSIONS

In this section, the reliability of the presented formulations and the developed computer program is confirmed first, then, the influence of various CEs on the free vibration characteristics of the nonlinearly tapered beam in different BCs is studied. For comparisons, the dimensions and physical constants of the beams studied are taken to be the same as those of Abrate (1995a) and Wu and Hsieh (2000): Total beam length L = 30.0 in, minimum height h_0 = 1.5 in, minimum width b_0 = 1 in, minimum cross-sectional area $A_0 = b_0 h_0$ = 1.5 in^2, minimum moment of inertia $I_0 = b_0 h_0^3/12 = 0.28125$ in^4, mass density $\rho = \rho_i = 0.73386 \times 10^{-3}$ lbm/in^3, Young's modulus $E = E_i = 30 \times 10^6$ psi, for i = 1~n. Furthermore, five *reference* parameters are introduced: reference lumped mass $m_{\text{ref}} = \rho A_0 L$ = 0.0330237 lbm, reference eccentricity $e_{\text{ref}} = 0.01L$ = 0.3 in, reference rotary inertia $J_{\text{ref}} = \rho A_0 L^3/1000$ = 0.02972133 lb$_m$-in^2, reference translational spring constant $k_{t,\text{ref}} = E_1 I_0/L^3 = 3.125 \times 10^2$ lb$_f$/in, and reference rotational spring constant $k_{r,\text{ref}} = E_1 I_0/L = 2.8125 \times 10^5$ lb$_f$-in/rad. In the foregoing expressions, the subscript 1 refers to the 1st beam segment.

1. Reliability of Presented Formulations and Developed Computer Program

In this subsection, the lowest five frequency coefficients $(\beta_r L)^2$ (r = 1~5) of the nonlinearly tapered clamped-pinned (C-P) beam without carrying any CEs are determined and shown

Table 1. The lowest five non-dimensional frequency coefficients ($\beta_r L$) (r = 1~5) for a nonlinearly tapered C-P beam without carrying any CEs (cf. Fig. 3) obtained from the presented CTMMc (with total number of beam segments n = 2) and FEM (with total number of beam elements n_e = 300), and the existing literature, with taper constants: (a) α = 0.0, (b) α = ±1.0, (c) α = ±2.0.

(a) α = 0.0

Methods	α	Frequency coefficients, $(\beta_r L)^2$					[a]CPU time (sec)
		$(\beta_1 L)^2$	$(\beta_2 L)^2$	$(\beta_3 L)^2$	$(\beta_4 L)^2$	$(\beta_5 L)^2$	
Exact (Abrate, 1995a)	0.0	15.4182	49.9649	104.248	178.270	272.032	—
ANCM (Wu et al., 2000)		15.4186	49.9654	104.247	178.269	272.031	—
FEM		15.4182	49.9649	104.248	178.270	272.031	140.9
CTMMc		15.4182	49.9649	104.248	178.270	272.031	0.03

[a] On an ASUS MD750 PC with Intel Core i7-3770CPU

(b) α = ±1.0

Methods	α	Frequency coefficients, $(\beta_r L)^2$					[a]CPU time (sec)
		$(\beta_1 L)^2$	$(\beta_2 L)^2$	$(\beta_3 L)^2$	$(\beta_4 L)^2$	$(\beta_5 L)^2$	
Exact (Abrate, 1995a)	1.0	12.3635	47.6265	102.025	176.105	269.904	—
ANCM (Wu et al., 2000)	1.0	12.3633	47.6259	102.025	176.105	269.901	—
	-1.0[b]	12.3633	47.6259	102.025	176.105	269.901	—
FEM	1.0	12.3636	47.6267	102.025	176.106	269.901	153.9
CTMMc	1.0	12.3635	47.6265	102.025	176.105	269.900	0.03
	-1.0[b]	12.3635	47.6265	102.025	176.105	269.900	0.03

[a] On an ASUS MD750 PC with Intel Core i7-3770CPU
[b] For the beam with P-C BCs

(c) α = ±2.0

Methods	α	Frequency coefficients, $(\beta_r L)^2$					[a]CPU time (sec)
		$(\beta_1 L)^2$	$(\beta_2 L)^2$	$(\beta_3 L)^2$	$(\beta_4 L)^2$	$(\beta_5 L)^2$	
Exact (Abrate, 1995a)	2.0	10.5984	46.6678	101.174	175.304	269.136	—
ANCM (Wu et al., 2000)	2.0	10.5986	46.6673	101.174	175.304	269.129	—
	-2.0[b]	10.5986	46.6673	101.174	175.304	269.129	—
FEM	2.0	10.5985	46.6681	101.174	175.305	269.130	154.3
CTMMc	2.0	10.5984	46.6678	101.174	175.304	269.128	0.03
	-2.0[b]	10.5984	46.6678	101.174	175.304	269.128	0.03

[a] On an ASUS MD750 PC with Intel Core i7-3770CPU
[b] For the beam with P-C BCs

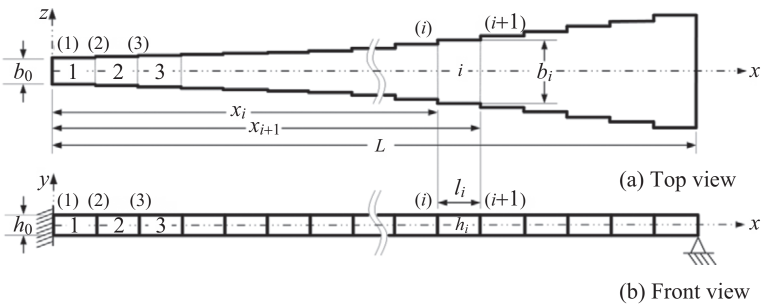

Fig. 3. The finite element model for the nonlinearly tapered clamped-pinned (C-P) beam with *positive* taper constant and without carrying any CEs.

in Table 1(a) for the case of taper constant α = 0; Table 1(b) for α = ±1.0; and Table 1(c) for α = ±2.0. In addition to the results of the presented CTMMc (with total number of beam segments n = 2), those of Abrate (1995a), Wu and Hsieh (2000), and the conventional FEM (with total number of beam elements n_e = 300) are also listed in Table 1.

The corresponding FEM model is shown in Fig. 3, where the entire tapered beam is replaced by a stepped beam composed of

Table 2. Influence of various BCs on the lowest five natural frequencies $\omega_r (r = 1\sim5)$ of the nonlinearly tapered beam with taper constant α = 0.5 and without carrying any CEs (cf. Fig. 3), obtained from presented CTMMc and CTMMn (with total number of beam segments n = 2) and FEM (with total number of beam elements n_e = 300), and the existing literature.

BCs	Methods	Natural frequencies, ω_r (rad/sec)					CPU Time (sec)
		ω_1	ω_2	ω_3	ω_4	ω_5	
F-F	FEM	2248.5407	6095.1132	11866.0825	19552.0555	29156.3853	149.6
	[a]CTMMc	2248.5461	6095.1280	11866.1115	19552.1034	29156.4566	0.03
C-C	FEM	2176.4161	5999.3746	11761.1729	19441.8162	29042.7193	146.3
	CTMMc	2176.4160	5999.3745	11761.1727	19441.8160	29042.7195	0.03
	[b]CTMMn	2176.4160	5999.3745	11761.1727	19441.8160	29042.7189	0.34
P-P	[c]ANCM	935.8919	3862.9643	8676.9179	15404.4470	24049.5986	—
	FEM	935.8803	3862.9589	8676.8623	15404.4807	24049.5401	151.7
	CTMMc	935.8814	3862.9637	8676.8730	15404.4996	24049.5696	0.03
	CTMMn	935.8814	3862.9637	8676.8730	15404.4996	24049.5696	0.28
P-C	ANCM	1657.7654	5028.6545	10317.0580	17522.0588	26645.3397	—
	FEM	1657.7492	5028.6023	10317.0444	17521.8663	26645.3351	150.6
	CTMMc	1657.7552	5028.6207	10317.0824	17521.9308	26645.4333	0.03
	CTMMn	1657.7552	5028.6207	10317.0823	17521.9308	26645.4332	0.31
C-P	ANCM	1327.5922	4716.8123	10001.9291	17204.9487	26327.1998	—
	FEM	1327.5957	4716.8673	10001.8762	17204.9748	26327.2683	147.7
	CTMMc	1327.5920	4716.8553	10001.8512	17204.9319	26327.2029	0.03
	CTMMn	1327.5920	4716.8553	10001.8511	17204.9319	26327.2028	0.31
C-F	ANCM	203.8352	1835.6157	5727.5757	11491.7806	19175.0754	—
	FEM	203.8463	1835.5870	5727.5866	11491.7411	19175.1913	148.4
	CTMMc	203.8456	1835.5770	5727.5576	11491.6836	19175.0958	0.03
	CTMMn	203.8456	1835.5770	5727.5576	11491.6836	19175.0958	0.23
F-C	ANCM	547.6202	2496.3165	6363.3976	12131.2240	19816.2456	—
	FEM	547.6192	2496.3006	6363.4199	12131.0661	19816.1595	147.9
	CTMMc	547.6225	2496.3178	6363.4656	12131.1545	19816.3047	0.03
	CTMMn	547.6225	2496.3178	6363.4655	12131.1544	19816.3046	0.25

[a] From the presented CTMM based on *classical* BCs.
[b] From the presented CTMM based on *non-classical* BCs.
[c] From Wu and Hsieh (2000).

300 uniform beam elements. The cross-sectional area A_i and the moment of inertia I_i for the ith *uniform* beam element are equal to the average values of the corresponding ones for the ith *tapered* beam element, respectively, i.e.

$$A_i = A_0(\varepsilon + \bar{\alpha}\,\tilde{x}_i)^4,\ I_i = I_0(\varepsilon + \bar{\alpha}\,\tilde{x}_i)^4 \qquad (65a, b)$$

with

$$\tilde{x}_i = (x_i + x_{i+1})/2 \qquad (66)$$

The mass per unit length of the ith *uniform* beam element is evaluated by ρA_i, and the length of each *uniform* beam element is given by $l_i = L/n = 30/300 = 0.1$ in. From Tables 1(a)-(c) one finds that: (i) The results of CTMMc and FEM are all very close to the solutions given by Abrate (1995a) and Wu and Hsieh (2000), but the accuracy of CTMMc is better than that of FEM, particularly for the beam with higher taper constant α. (ii) The values of $(\beta_r L)^2$ obtained from the C-P beam with *positive* taper constant $\alpha = +1.0, +2.0$ are exactly equal to those obtained from the P-C beam with *negative* taper constant $\alpha = -1.0, -2.0$. (iii) In each case, the CPU time (on an ASUS MD750 PC with Intel Core i7-3770CPU) required by the presented CTMMc is less than 0.01% of that required by the conventional FEM.

The influence of various BCs on the lowest five natural frequencies ω_r ($r = 1\sim5$) of the nonlinearly tapered beam with taper constant $\alpha = 0.5$ and *without* carrying any CEs obtained from ANCM (Wu and Hsieh, 2000), FEM, CTMMc and CTMMn are shown in Table 2, and the corresponding five unit-amplitude mode shapes for the beam with P-P, F-C and P-C BCs are shown in Fig. 4.

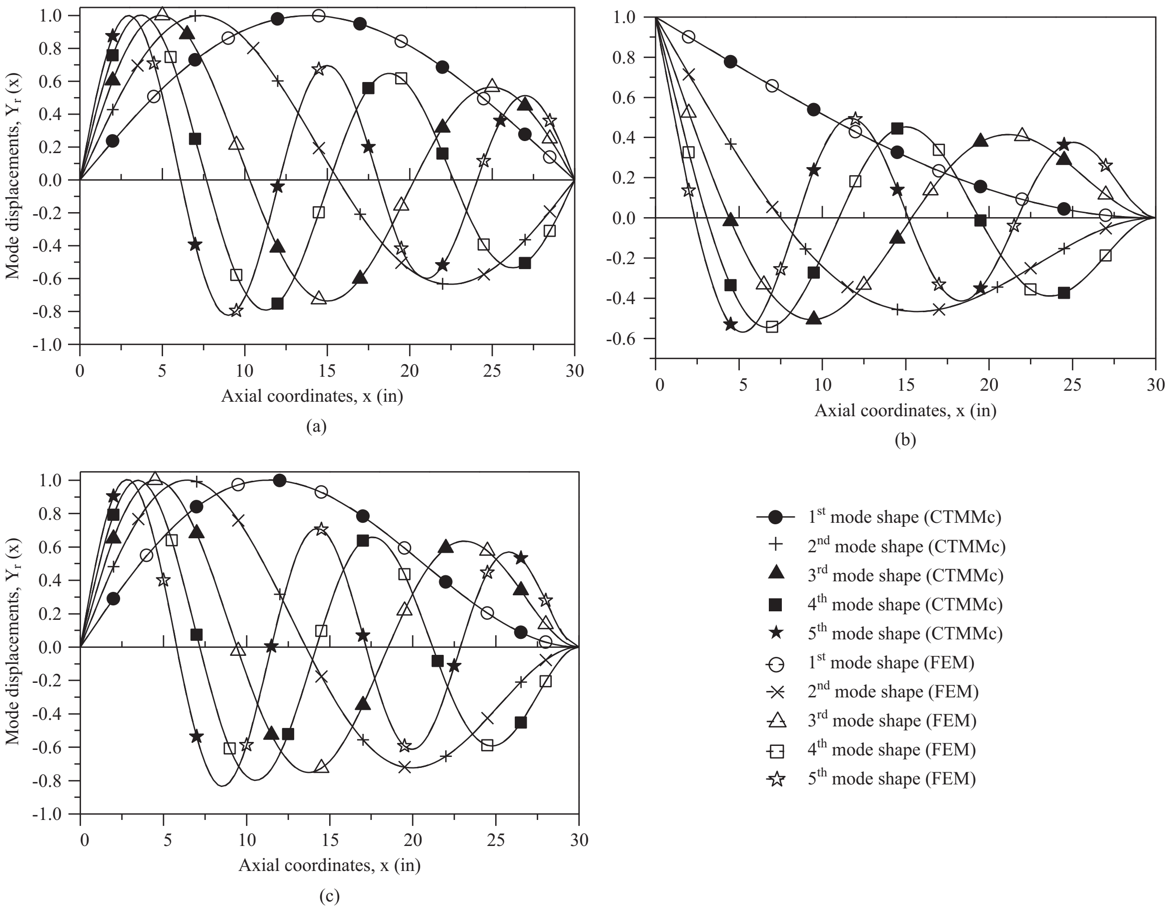

Fig. 4. The lowest five unit-amplitude mode shapes of the nonlinearly tapered beam with taper constant α = 0.5 and without carrying any CEs (Fig. 3), and with corresponding natural frequencies showing in Table 2 in the (a) P-P, (b) F-C and (c) P-C BCs, respectively.

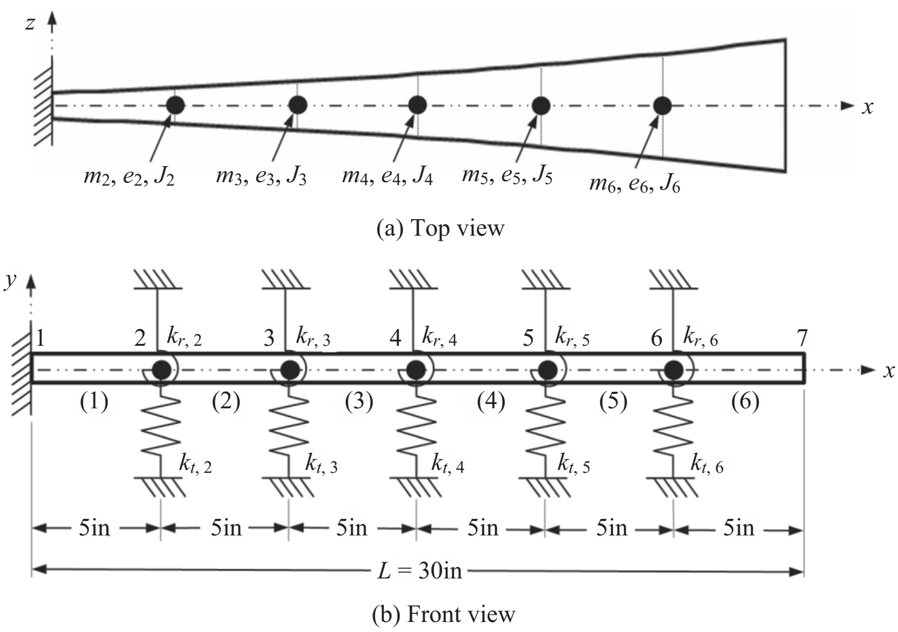

Fig. 5. A nonlinearly tapered clamped-free (C-F) beam with taper constant α = 0.5 and carrying five identical sets of CEs, with each set of CEs consisting of a lumped mass m_i (with eccentricity e_i and rotary inertia J_i), a translational spring with stiffness $k_{t,i}$ and a rotational spring with stiffness $k_{r,i}$ (i = 2 – 6).

Table 3. Influence of loading conditions on the lowest four natural frequencies ω_r (r = 1~4) of the nonlinearly tapered clamped-free (C-F) beam with taper constant α = 0.5 and carrying five identical sets of CEs as shown in Fig. 5, obtained from the presented CTMMc (with total number of beam segments n = 6) and FEM (with total number of beam elements n_e = 300).

Cases	[a]Concentrated elements						Methods	Natural frequencies, ω_r (rad/sec)			
	Positions	Lumped masses			Elastic springs						
	x_i/L	m_i^*	e_i^*	J_i^*	$k_{t,i}^*$	$k_{r,i}^*$		ω_1	ω_2	ω_3	ω_4
0	0 (No CEs)	0	0	0	0	0	CTMMc	203.8456	1835.5770	5727.5576	11491.6836
							FEM	203.8463	1835.5870	5727.5866	11491.7411
1	1/2 (i = 4)	1	0	0	0	0	CTMMc	191.1861	1383.1090	5706.7066	9585.9075
							FEM	191.1880	1383.1160	5706.7350	9585.9546
2		0	0	0	1	0.01	CTMMc	207.2377	1837.7833	5727.9811	11492.0218
							FEM	207.2587	1837.8074	5728.0102	11492.0815
3		1	0	0	1	0.01	CTMMc	194.4202	1384.4377	5707.1179	9585.9851
							FEM	194.4398	1384.4530	5707.1463	9586.0327
4	$\frac{1}{3}, \frac{1}{2}, \frac{2}{3}$ (i = 3, 4, 5)	1	0	0	0	0	CTMMc	166.5364	1180.2887	3611.6301	8028.8332
							FEM	166.5375	1180.2952	3611.6441	8028.8509
5		1	1	1	0	0	CTMMc	164.9117	1180.0765	3605.4710	7784.3177
							FEM	164.8947	1179.8750	3604.7695	7783.0255
6		1	1	0.1	1	0.01	CTMMc	174.8437	1186.8424	3642.0091	8041.9951
							FEM	174.8941	1186.8235	3641.8954	8041.7455
7	$\frac{1}{6}, \frac{2}{6}, \frac{3}{6}, \frac{4}{6}, \frac{5}{6}$ (i = 2, 3, 4, 5, 6)	1	0	0	0	0	CTMMc	140.7797	1103.8019	3257.5695	6296.8523
							FEM	140.7801	1103.8078	3257.5875	6296.8802
8		1	1	1	0	0	CTMMc	139.0921	1086.0881	3171.0649	6068.9015
							FEM	139.0714	1085.8593	3170.3331	6067.4498
9		1	1	0.1	1	0.01	CTMMc	156.3829	1098.1784	3232.4158	6246.4783
							FEM	156.4632	1098.1575	3232.2974	6245.9454

[a] $m_i^* = m_i/m_{\text{ref}}$, $e_i^* = e_i/e_{\text{ref}}$, $J_i^* = J_i/J_{\text{ref}}$, $k_{t,i}^* = k_{t,i}/k_{t,\text{ref}}$ and $k_{r,i}^* = k_{r,i}/k_{r,\text{ref}}$.

From Table 2 one finds that the results of CTMMc, CTMMn and FEM are very close to ANCM, and in each case, the CPU time required by the presented CTMMc (or CTMMn) is less than 0.2% of that required by the conventional FEM. In Fig. 4, the mode shapes obtained from CTMMc (or CTMMn) and FEM are denoted by the solid lines (—) and the dashed lines (- - -), respectively. In which, Figs. 4(a)-(c) are for the P-P, F-C and P-C beams, respectively. It is sees that the lowest five mode shapes obtained from the presented CTMMc (or CTMMn) are in good agreement with those obtained from FEM. Furthermore, for the rth mode shape (with $r \geq 2$), the mode displacement amplitude near the smallest (left) end of the beam is greater than that near the largest (right) end. This is a reasonable result, because the stiffness of the left end is much smaller than that of the right end for the nonlinearly tapered beam with α = +0.5 (cf. Fig. 2 or 3). It is noted that, in Figs. 4(a)-(c), the 1st, 2nd, 3rd, 4th and 5th mode shapes are denoted by the symbols, ● (or ○), + (or ×), ▲ (or △), ■ (or □) and ★ (or ☆), respectively.

2. Influence of Loading Conditions on Free Vibrations of a Nonlinearly Tapered C-F Beam Carrying Various CEs

The reliability of the presented formulations and the developed computer program has been confirmed in the last ***Subsection 6.1***, and the objective of this subsection is to study the influence of various CEs on the free vibration characteristics of a nonlinearly tapered C-F beam with taper constant α = 0.5 as shown in Fig. 5. The tapered beam carries five identical sets of CEs with each set of CEs consisting of a lumped mass m_i (with eccentricity e_i and rotary inertia J_i), a translational spring with stiffness $k_{t,i}$ and a rotational spring with stiffness $k_{r,i}$, for i = 2, 3, 4, 5 and 6. The lowest four natural frequencies of the beam for *ten cases* are shown in Table 3 and the associated lowest three mode shapes for three cases are plotted in Fig. 6.

The loading conditions for the ten cases are (cf. Table 3):

(a) In **Case 0**, the beam does not carry any CEs and it is the same as the C-F beam studied in Table 2. It is obvious that this case is only for comparisons.

(b) In **Cases 1-3**, the beam carries "one set" of CEs (located at node 4 with $x_i/L = x_4/L = 1/2$) consisting of a lumped mass with $m_4^* = m_4/m_{\text{ref}} = 1$ for **Case 1**; a translational spring with $k_{t,4}^* = k_{t,4}/k_{t,\mathrm{ref}} = 1$ and a rotational spring with $k_{r,4}^* = k_{r,4}/k_{r,\mathrm{ref}} = 0.01$ for **Case 2**; and a lumped mass with $m_4^* = m_4/m_{\mathrm{ref}} = 1$, a translational spring with $k_{t,4}^* = k_{t,4}/k_{t,\mathrm{ref}} = 1$ as well as a rotational spring with $k_{r,4}^* = k_{r,4}/k_{r,\mathrm{ref}} = 0.01$ for **Case 3**. Note that, in the present three cases (**Cases 1-3**), the lumped mass m_4 does not possess eccentricity and rotary inertia, i.e., $e_i = J_i = 0$ (for $i = 4$).

(c) In **Cases 4-6**, the beam carries "three sets" of CEs (located at nodes i with x_i/L = 1/3, 1/2 and 2/3, for i = 3, 4, 5, respectively) with each set of CEs consisting of a lumped mass with $m_i^* = m_i/m_{\mathrm{ref}} = 1$ (and $e_i = J_i = 0$) for **Case 4**; a lumped mass with $m_i^* = m_i/m_{\mathrm{ref}} = 1$ (possessing $e_i^* = e_i/e_{\mathrm{ref}} = 1$ and $J_i^* = J_i/J_{\mathrm{ref}} = 1$) for **Case 5**; and a lumped mass with $m_i^* = m_i/m_{\mathrm{ref}} = 1$ (possessing $e_i^* = e_i/e_{\mathrm{ref}} = 1$ and $J_i^* = J_i/J_{\mathrm{ref}} = 0.1$), a translational spring with $k_{t,i}^* = k_{t,i}/k_{t,\mathrm{ref}} = 1$ as well as a rotational spring with $k_{r,i}^* = k_{r,i}/k_{r,\mathrm{ref}} = 0.01$ for **Case 6**.

(d) In **Cases 7-9**, the beam carries "five sets" of CEs (located at nodes i with x_i/L = 1/6, 2/6, 3/6, 4/6 and 5/6, for i = 2, 3, 4, 5, 6, respectively) with each set of CEs consisting of a lumped mass with $m_i^* = m_i/m_{\mathrm{ref}} = 1$ (and $e_i = J_i = 0$) for **Case 7**; a lumped mass with $m_i^* = m_i/m_{\mathrm{ref}} = 1$ (possessing $e_i^* = e_i/e_{\mathrm{ref}} = 1$ and $J_i^* = J_i/J_{\mathrm{ref}} = 1$) for **Case 8**; and a lumped mass with $m_i^* = m_i/m_{\mathrm{ref}} = 1$ (possessing $e_i^* = e_i/e_{\mathrm{ref}} = 1$ and $J_i^* = J_i/J_{\mathrm{ref}} = 0.1$), a translational spring with $k_{t,i}^* = k_{t,i}/k_{t,\mathrm{ref}} = 1$ as well as a rotational spring with $k_{r,i}^* = k_{r,i}/k_{r,\mathrm{ref}} = 0.01$ for **Case 9**.

It is noted that the values of the five reference parameters have been shown at the beginning of this section, i.e., $m_{\mathrm{ref}} = \rho A_0 L$ = 0.0330237 $\mathrm{lb_m}$, $J_{\mathrm{ref}} = \rho A_0 L^3/1000$ = 0.02972133 $\mathrm{lb_m}$-in^2, $e_{\mathrm{ref}} = 0.01L$ = 0.3 in, $k_{t,\mathrm{ref}} = E_1 I_0/L^3$ = 3.125 × 10^2 $\mathrm{lb_f}$/in and $k_{r,\mathrm{ref}} = E_1 I_0/L$ = 2.8125 × 10^5 $\mathrm{lb_f}$-in/rad. Furthermore, Fig. 5 reveals that the entire tapered beam is subdivided into 6 beam segments with equal lengths $l_i = L/n = 30/6 = 5$ in (i = 1~6) and the locations for the five CEs are: x_2 = 5 in, x_3 = 10 in, x_4 = 15 in, x_5 = 20 in and x_6 = 25 in. Form Table 3 one sees that:

(i) All natural frequencies obtained from CTMMc (with n = 6) are very close to the corresponding ones obtained from FEM (with n_e = 300).

(ii) Among **Cases 1-3**, the lowest four natural frequencies (ω_1 to ω_4) of **Case 1** for the beam carrying a "lumped mass" only are *lower* than those of the other cases; the values of "ω_1 to ω_4" of **Case 2** for the beam carrying "elastic elements" (a translational spring as well as a rotational spring) only are *higher* than those of the other cases; and the values of "ω_1 to ω_4" of **Case 3** for the beam carrying a "lumped mass" and two "elastic elements" are *middle*. The last phenomenon is reasonable, because the "lumped mass" can raise the inertia effect (and reduce the natural frequencies of the beam), but the "elastic elements" can raise the stiffness (and raise the natural frequencies).

(iii) Among **Cases 4-6**, the lowest four natural frequencies (ω_1 to ω_4) of **Case 6** for the beam carrying three lumped masses (possessing eccentricities and rotary inertias), three translational springs and three rotational springs are *higher* than those of the other cases; the values of "ω_1 to ω_4" of **Case 5** for the beam carrying three lumped masses (possessing eccentricities and rotary inertias) are *lower* than those of the other cases; and the values of "ω_1 to ω_4" of **Case 4** for the beam carrying three lumped masses (no eccentricities and rotary inertias) only are *middle*. The last results are also reasonable, because the "eccentricities and rotary inertias" in **Case 5** have the effect of increasing inertia and, in turn, reducing the natural frequencies.

(iv) Similarly to (iii), among **Cases 7-9** for the beam carrying "five sets" of CEs, the lowest four natural frequencies of **Case 9** for the beam carrying five lumped masses (possessing eccentricities and rotary inertias), five translational springs and five rotational springs are *higher* than those of **Case 7** or **8** for the beam carrying five "lumped masses" and no "elastic CEs".

In addition to the lowest four natural frequencies listed in Table 3, the lowest three unit-amplitude mode shapes are shown in Fig. 6(a) for the beam carrying "no" CEs (**Case 0**), in Fig. 6(b) for the beam carrying "three sets" of CEs (**Case 6**) and in Fig. 6(c) for the beam carrying "five sets" of CEs (**Case 9**). It is seen that: (i) The mode shapes obtained from the presented CTMMc (denoted by solid curves, —) are very close to the corresponding ones obtained from FEM (denoted by dashed curves, - - -). (ii) The mode displacements of 1st mode shape for **Case 0** are very *close* to the corresponding ones for **Case 6** or **Case 9**. (iii) The mode displacement amplitudes of the 2nd and 3rd mode shapes for **Case 0** are *greater* than the corresponding ones for **Case 6** or **Case 9**. The reason for the last result is: Among the various CEs, the *lumped masses* can raise the inertia effect and the *elastic springs* can raise the stiffness of the beam segments attached by the CEs, so that the mode displacement amplitudes of the 2nd and 3rd mode shapes for the beam carrying three sets of CEs (**Case 6**) or five sets of CEs (**Case 9)** near its middle are *smaller* than the corresponding ones for the beam carrying no CEs (**Case 0**).

3. Free Vibration Analysis for a Nonlinearly Tapered Beam Carrying Arbitrarily Distributed CEs with "Non-Classical" BCs

The objective of this subsection is to show the availability

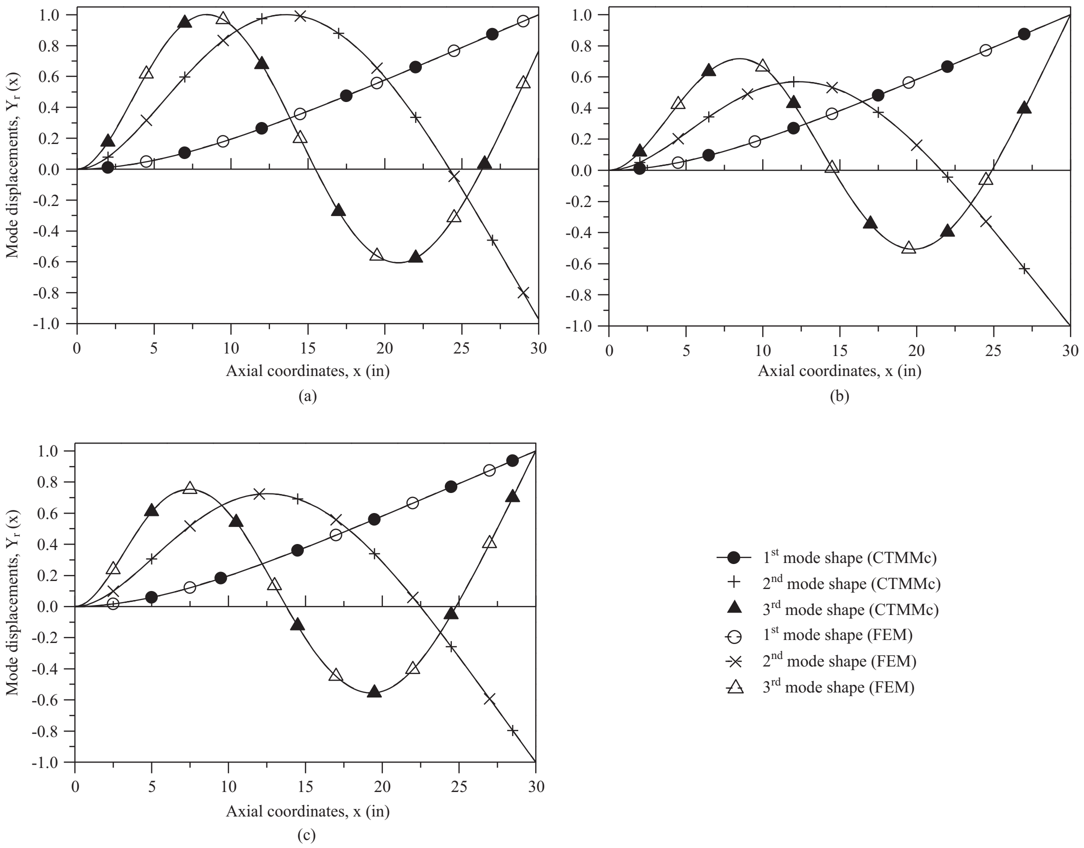

Fig. 6. The lowest three unit-amplitude mode shapes of the nonlinearly tapered C-F beam with taper constant α = 0.5 and carrying (cf. Fig. 5): (a) no CEs (Case 0), (b) three sets of CEs (Case 6), and (c) five sets of CEs (Case 9), with corresponding natural frequencies shown in Table 3.

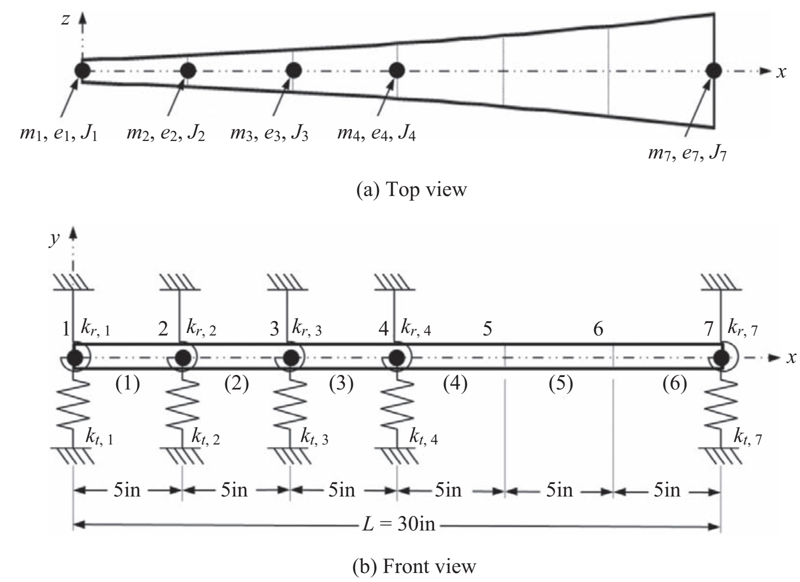

Fig. 7. A nonlinearly tapered free-free (F-F) beam with taper constantα = 0.5 and carrying five identical sets of CEs with each set CEs consisting of a lumped mass m_i (possessing eccentricity e_i and rotary inertia J_i), a translational spring with stiffness $k_{t,i}$ and a rotational spring with stiffness $k_{r,i}$.

of CTMM for a nonlinearly tapered beam carrying arbitrarily distributed CEs in various "non-classical" BCs. Fig. 7 shows the beam with taper constant α = 0.5 studied. It carries five *identical* sets of CEs located at nodes i = 1, 2, 3, 4, and 7, with x_i/L = 0, 1/6, 2/6, 3/6 and 1 (or x_1 = 0, x_2 = 5 in, x_3 = 10 in, x_4 = 15 in and x_7 = 30 in), respectively. In which, each set of CEs

Table 4. Influence of BCs on the lowest five natural frequencies ω_r (r = 1~5) of the nonlinearly tapered beam with taper constant α = 0.5 and carrying five identical sets of CEs located at x_i/L = 0, 1/6, 2/6, 3/6 and 1.0 as shown in Fig. 7, obtained from presented CTMMn (with n = 6 n = 6) and FEM (with n_e = 300).

BCs	Methods	Natural frequencies, ω_r (rad/sec)					CPU
		ω_1	ω_2	ω_3	ω_4	ω_5	Time (sec)
[a]C-C	CTMMn	1230.6690	3718.0547	7330.8713	10736.7315	22908.2466	0.11
	FEM	1230.6320	3717.9062	7330.5805	10736.2428	22903.5206	145.5
P-P	CTMMn	561.5011	2461.5869	5371.4304	8922.5783	18416.5667	0.08
	FEM	561.5446	2462.0919	5375.3774	8929.6556	18494.9728	149.2
C-P	CTMMn	849.0018	3061.0385	6001.4714	9448.5072	18507.1143	0.09
	FEM	849.0659	3061.9474	6006.2240	9454.6017	18587.1568	146.1
P-C	CTMMn	886.8868	3026.6768	6621.2833	10459.0230	22648.0267	0.11
	FEM	886.8663	3026.5363	6621.0069	10458.5722	22659.1879	147.7
F-C	CTMMn	234.3695	1156.1083	3369.6417	6859.8844	10540.0128	0.06
	FEM	234.5110	1156.0572	3369.4540	6859.5622	10539.5362	144.9

[a] CTMMc is also available for the C-C beam.

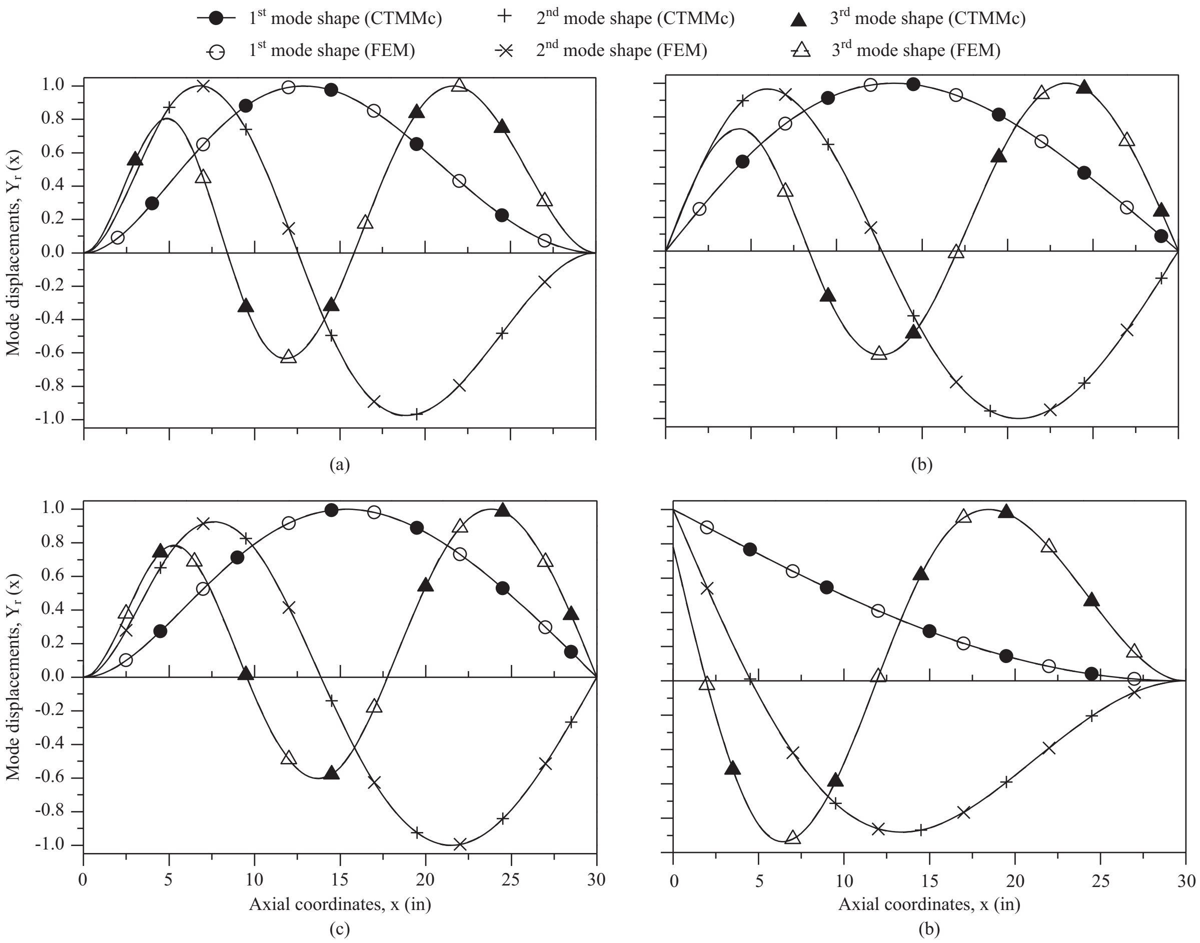

Fig. 8. The lowest three unit-amplitude mode shapes of the nonlinearly taper beam with taper constant α = 0.5, carrying five identical sets of CEs (cf. Fig. 7) and corresponding natural frequencies shown in Table 4 in the (a) C-C, (b) P-P, (c) C-P and (d) F-C BCs, respectively.

consists of a lumped mass with $m_i^* = m_i/m_{\mathrm{ref}} = 1$ (possessing eccentricity $e_i^* = e_i/e_{\mathrm{ref}} = 1$ and rotary inertia $J_i^* = J_i/J_{\mathrm{ref}} = 0.1$), a translational spring with $k_{t,i}^* = k_{t,i}/k_{t,\mathrm{ref}} = 1$ as well as a rotational spring with $k_{r,i}^* = k_{r,i}/k_{r,\mathrm{ref}} = 0.01$. Table 4 shows the values of ω_r (r = 1~5) of the nonlinear tapered beam in five BCs obtained from the presented CTMMn (with n = 6) and FEM (with n_e = 300), and Fig. 8 shows the lowest three unit-amplitude mode shapes for the beam in four BCs. Form Table 4 one sees that: (i) In various BCs, the lowest five natural frequencies obtained from CTMMn are very close to the corresponding ones obtained from FEM, particularly for the lowest two frequencies, ω_1 and ω_2. (ii) Among the five BCs, the lowest five natural frequencies of the F-C beam are *lowest* and those of C-C beam are *highest*, this is because the stiffness of the F-C beam is lowest and that of the C-C beam is highest. (iii) The lowest five natural frequencies of the P-P beam are *greater* than the corresponding ones of the F-C beam and *smaller* than those of the C-P beam, this is because the stiffness of P-P beam is greater than that of F-C beam and smaller than that of C-P beam. (iv) In each case, the CPU time required by the CTMMn is less 0.1% of that required by the conventional FEM.

The lowest three unit-amplitude mode shapes of the tapered beam with C-C, P-P, C-P and F-C BCs are shown in Figs. 8(a)-(d), respectively. It is similarly to Fig. 6 that the mode shapes obtained from CTMMn are represented by the solid curves (—) and those obtained from FEM are represented by the dashed curves (- - -), and the overlap each other between the corresponding solid and dashed curves confirms the good agreement between the results obtained from CTMMn and FEM. Furthermore, for the beam with C-C, P-P or C-P BCs shown in Figs. 8(a)-(c), respectively, the mode displacement amplitudes of the 2^{nd} and 3^{rd} mode shapes near the smallest (left) end of the beam are *smaller* than those near the largest (right) end, and this trend is opposite to that for the same tapered P-P or P-C beam carrying no CEs shown in Fig. 4(a) or (c). The last phenomenon is due to the fact that, in Fig. 7, the most CEs are near the smallest (left) end of the entire beam and they can raise the inertia effect and the stiffness of the beam segments near the smallest (left) end, so that the mode displacement amplitudes of the 2^{nd} and 3^{rd} mode shapes near the smallest (left) end are *smaller* than those near the largest (right) end of the C-C, P-P or C-P beam.

It is noted that the BCs for the F-F beam shown in Fig. 7 are "non-classical", thus, all results shown in Table 4 and Fig. 8 are obtained from CTMMn (based on the *non-classical* BCs), and only the natural frequencies and mode shapes for the beam with its two ends clamped can be obtained from CTMMc (based on the *classical* BCs). It is evident that, in Fig. 7, the effects of all CEs located at the two ends are nil, when the beam is in the C-C BCs.

VII. CONCLUSIONS

1. Based on the theory of continuous-mass transfer matrix method (CTMM), this paper has presented a formulation for determining the lowest several *exact* natural frequencies and associated mode shapes of a *nonlinearly* tapered beam carrying various concentrated elements (CEs) in the arbitrary boundary conditions (BCs). Numerical examples reveal that the results of the presented approach are very close to those of the FEM. Because the solutions of presented method are *exact*, they may be the benchmarks for evaluating the accuracy of the other *approximate* solutions, such as those of FEM or DQEM (differential quadrature element method).
2. In each of the cases studied in this paper, the CPU time required by the presented method is less than 0.2% of that required by the FEM, this is because the presented method needs only a few beam segments for achieving the *exact* solutions and the order of the characteristic-equation matrix keeps constant (4 × 4).
3. For the rth mode shape (with $r \geq 2$) of a nonlinearly tapered beam *without* carrying any CEs, the mode displacement amplitude near the smallest end is *greater* than that near the largest end, because the *flexural rigidity* of the tapered beam near the smallest end is less than that near the largest end.
4. For a nonlinearly tapered beam carrying multiple sets of CEs in various BCs, since each set of CEs (consisting of one lumped mass and two elastic springs) can raise both the inertia effect and the stiffness of the beam segments attached by them, the mode displacement amplitude of the rth mode shape (with $r \geq 2$) near the beam segment attached by the CEs is *smaller* than that of the beam segment without attaching to the CEs. Furthermore, in each set of CEs, the lumped mass has the effect of reducing the natural frequencies of the entire tapered beam and the elastic springs have reverse effect.
5. The free vibration problem for a tapered beam with both ends carrying various CEs in the *arbitrary* BCs can be solved with the CTMMn (on the basis of *non-classical* BCs) presented in this paper, however, only that in the *clamped-clamped* BCs can be solved with the CTMMc (on the basis of *classical* BCs) presented in the existing literature.
6. For a *nonlinearly* tapered beam carrying various CEs, including lumped masses (with eccentricities and rotary inertias), translational springs and rotational springs, the influence of the CEs on its lowest several natural frequencies and mode shapes in the *arbitrary* BCs is complicated, in such a case, the approach presented in this paper is useful for solving the last complicated problem.
7. The presented theories regarding the influence of the CEs and the non-classical (or non-zero) BCs on the free vibration characteristics of a nonlinearly tapered beam are useful for the development of the vortex wind turbine.

APPENDIX A

Transformation Displacement Functions Associated with Translational and Rotational CEs, $\bar{Y}(x)$ and $\bar{Y}'(x)$

If m_{eq} denotes the mass on the *equivalent* uniform beam associated with the actual mass m, then

$$m_{eq}\ddot{v}(x,t) = m\ddot{y}(x,t) \tag{A.1}$$

thus

$$m_{eq} = \frac{m\ddot{y}(x,t)}{\ddot{v}(x,t)} = \frac{m\ddot{y}(x,t)}{\varphi(x)\ddot{y}(x,t)} = \frac{m}{\varphi(x)} \tag{A.2}$$

and

$$m_{eq}\ddot{y}(x,t) = \frac{m}{\varphi(x)}\left(\frac{\ddot{v}(x,t)}{\varphi(x)}\right) = m\left(\frac{\ddot{v}(x,t)}{\varphi^2(x)}\right) \tag{A.3}$$

For free vibrations, one has

$$y(x,t) = \bar{Y}(x)e^{j\omega t}\ ,\ v(x,t) = V(x)e^{j\omega t} \tag{A.4a, b}$$

Where $\bar{Y}(x)$ and $V(x)$ denote the amplitudes of $y(x,t)$ and $v(x,t)$, respectively, ω is natural frequency of the "loaded" beam (carrying any CEs), and $j = \sqrt{-1}$.

From Eqs. (A.3) and (A.4), one obtains

$$m_{eq}\bar{Y}(x)\omega^2 = m[V(x)/\varphi^2(x)]\omega^2 \tag{A.5}$$

The above equation indicates that if one sets $m_{eq} = m$ and

$$\bar{Y}(x) = V(x)/\varphi^2(x) \tag{A.6}$$

then $m\bar{Y}(x)\omega^2 = m[V(x)/\varphi^2]\omega^2$ denotes the *inertial force* on the (equivalent) uniform beam due to the *concentrated mass m*. Similarly, the *elastic* (*restoring*) *moment* on the (equivalent) uniform beam due to the *concentrated rotational spring* k_r is given by

$$k_r\bar{Y}' = k_r\left[\frac{V'(x)\varphi^2(x) - 2\varphi(x)\varphi'(x)V(x)}{\varphi^4(x)}\right]$$

or

$$\bar{Y}' = \frac{V'(x)\varphi^2(x) - 2\varphi(x)\varphi'(x)V(x)}{\varphi^4(x)} \tag{A.7}$$

APPENDIX B

Classical BCs for Nonlinearly Tapered Beam

The BCs for a beam without any CEs attached to its ends are called the "classical" BCs and these BCs for three beams are derived in this appendix: (i) free-free (F-F), (ii) pinned-pinned (P-P) and (iii) clamped-clamped (C-C) beams.

(i) BCs for the F-F Beam

For a F-F beam, the BCs at the *left* end of the entire beam (i.e., *left* end of the 1st beam segment) are given by

$$Y_1''(0) = 0\ ,\ Y_1'''(0) = 0 \tag{A.8a, b}$$

From Eqs. (12), (15), (16) and (A.8a,b), one can obtain the corresponding BCs for the function $V_1(0)$ to be

$$V_1''(0)+6\lambda^2V_1(0)-4\lambda V_1'(0)=0 \tag{A.9a}$$

$$V_1'''(0)+12\lambda^3V_1(0)-6\lambda^2V_1'(0)=0 \tag{A.9b}$$

where

$$\lambda=\bar{\alpha}/\varepsilon \tag{A.9c}$$

Substituting the function $V(x)$ given by Eq. (14) into Eqs. (A.9a,b), one obtains

$$S_{11}A_1+S_{12}B_1+S_{13}C_1+S_{14}D_1=0 \tag{A.10a}$$

$$S_{21}A_1+S_{22}B_1+S_{23}C_1+S_{24}D_1=0 \tag{A.10b}$$

where

$$S_{11}=12\lambda^2,\ S_{12}=-2\beta_1^2,\ S_{13}=-8\lambda\beta_1,\ S_{14}=0 \tag{A.11a-d}$$

$$S_{21}=24\lambda^3,\ S_{22}=0,\ S_{23}=-12\lambda^2\beta_1,\ S_{24}=-2\beta_1^3 \tag{A.12a-d}$$

Similarly, the BCs at *right* end of the entire F-F beam (i.e., at *right* end the *n*th beam segment) are given by

$$Y_n''(L)=0,\ Y_n'''(L)=0 \tag{A.13a, b}$$

From Eqs. (12), (15), (16) and (A.13a,b), one obtains

$$V_n''(L)+6\mu^2V_n(L)-4\mu V_n'(L)=0 \tag{A.14a}$$

$$V_n'''(L)+12\mu^3V_n(L)-6\mu^2V_n'(L)=0 \tag{A.14b}$$

where

$$\mu=\frac{\bar{\alpha}}{(\varepsilon+\bar{\alpha}L)} \tag{A.14c}$$

The substitution of $V(x)$ given by Eq. (14) into Eq. (A.14a,b) produces

$$U_{11}A_n+U_{12}B_n+U_{13}C_n+U_{14}D_n=0 \tag{A.15a}$$

$$U_{21}A_n+U_{22}B_n+U_{23}C_n+U_{24}D_n=0 \tag{A.15b}$$

where

$$U_{11}=-[\beta_n^2-6\mu^2]\cos\beta_nL+[\beta_n^2+6\mu^2]\cosh\beta_nL-4\mu\beta_n(-\sin\beta_nL+\sinh\beta_nL) \tag{A.16a}$$

$$U_{12}=-[\beta_n^2-6\mu^2]\cos\beta_nL-[\beta_n^2+6\mu^2]\cosh\beta_nL-4\mu\beta_n(-\sin\beta_nL-\sinh\beta_nL) \tag{A.16b}$$

$$U_{13} = -[\beta_n^2 - 6\mu^2]\sin\beta_n L + [\beta_n^2 + 6\mu^2]\sinh\beta_n L - 4\mu\beta_n(\cos\beta_n L + \cosh\beta_n L) \tag{A.16c}$$

$$U_{14} = -[\beta_n^2 - 6\mu^2]\sin\beta_n L - [\beta_n^2 + 6\mu^2]\sinh\beta_n L - 4\mu\beta_n(\cos\beta_n L - \cosh\beta_n L) \tag{A.16d}$$

$$U_{21} = \beta_n[\beta_n^2 + 6\mu^2]\sin\beta_n L + \beta_n[\beta_{n1}^2 - 6\mu^2]\sinh\beta_n L + 12\mu^3(\cos\beta_n L + \cosh\beta_n L) \tag{A.17a}$$

$$U_{22} = \beta_n[\beta_n^2 + 6\mu^2]\sin\beta_n L - \beta_n[\beta_n^2 - 6\mu^2]\sinh\beta_n L + 12\mu^3(\cos\beta_{n+1} L - \cosh\beta_{n+1} L) \tag{A.17b}$$

$$U_{23} = -\beta_n[\beta_n^2 + 6\mu^2]\cos\beta_n L + \beta_n[\beta_n^2 - 6\mu^2]\cosh\beta_n L + 12\mu^3(\sin\beta_n L + \sinh\beta_n L) \tag{A.17c}$$

$$U_{24} = -\beta_n[\beta_n^2 + 6\mu^2]\cos\beta_n L - \beta_n[\beta_{n1}^2 - 6\mu^2]\cosh\beta_n L + 12\mu^3(\sin\beta_n L - \sinh\beta_n L) \tag{A.17d}$$

(ii) BCs for the P-P Beam

The BCs at *left* end of the entire P-P beam are given by

$$Y_1(0) = 0\,,\ Y_1''(0) = 0 \tag{A.18a, b}$$

From Eqs. (12), (15), (16) and (A.18a, b), one obtains

$$V_1(0) = \varphi_1(0)Y_1(0) = 0\,,\ V_1''(0) - 4\lambda V_1'(0) = 0 \tag{A.19a, b}$$

Substituting Eq. (14) into Eqs. (A.19a, b), one can obtain two equations to take the forms like Eqs. (A.10a, b) with the coefficients of the constants A_1, B_1, C_1 and D_1 given by

$$S_{11} = 2\,,\ S_{12} = S_{13} = S_{14} = 0 \tag{A.20a-d}$$

$$S_{21} = 0\,,\ S_{22} = -2\beta_1^2\,,\ S_{23} = -8\lambda\beta_1\,,\ S_{24} = 0 \tag{A.21a-d}$$

Similarly, the BCs at *right* end of the entire P-P beam are given by

$$Y_n(L) = 0\,,\ Y_n''(L) = 0 \tag{A.22a, b}$$

From Eqs. (12), (15), (16) and (A.22a, b), can obtains

$$V_n(L) = \varphi_n(L)Y_n(L) = 0\,,\ V_n''(L) - 4\mu V_n'(L) = 0 \tag{A.23a, b}$$

Substituting Eq. (14) into Eqs. (A.23a, b), one can obtain two equations to take the forms like Eqs. (A.15a, b) with the coefficients of the constants A_n, B_n, C_n and D_n given by

$$U_{11} = \cos\beta_n L + \cosh\beta_n L\,,\ U_{12} = \cos\beta_n L - \cosh\beta_n L \tag{A.24a, b}$$

$$U_{13} = \sin\beta_n L + \sinh\beta_n L\,,\ U_{14} = \sin\beta_n L - \sinh\beta_n L \tag{A.24c, d}$$

$$U_{21} = \beta_n^2(-\cos\beta_n L + \cosh\beta_n L) - 4\mu\beta_n(-\sin\beta_n L + \sinh\beta_n L) \tag{A.25a}$$

$$U_{22} = \beta_n^2(-\cos\beta_n L - \cosh\beta_n L) - 4\mu\beta_n(-\sin\beta_n L - \sinh\beta_n L) \tag{A.25b}$$

$$U_{23} = \beta_n^2(-\sin\beta_n L + \sinh\beta_n L) - 4\mu\beta_n(\cos\beta_n L + \cosh\beta_n L) \tag{A.25c}$$

$$U_{24} = \beta_n^2(-\sin\beta_n L - \sinh\beta_n L) - 4\mu\beta_n(\cos\beta_n L - \cosh\beta_n L) \tag{A.25d}$$

(iii) BCs for the C-C Beam

The BCs at *left* end of the entire C-C beam are given by

$$Y_1(0) = 0\ ,\ Y_1'\ (0) = 0 \tag{A.26a,b}$$

From Eqs. (12), (15), (16) and (A.26a, b), one obtains

$$V_1(0) = \varphi_1(0)Y_1(0) = 0\ ,\ V_1'(0) = \varphi_1'Y_1(0) + \varphi_1 Y_1'(0) = 0 \tag{A.27a,b}$$

Substituting Eq. (14) into Eq. (A.27a, b), one can obtain two equations to take the same forms as Eqs. (A.10a, b) with the coefficients of the constants A_1, B_1, C_1 and D_1 given by

$$S_{11} = 2\ ,\ S_{12} = S_{13} = S_{14} = 0 \tag{A.28a-d}$$

$$S_{21} = 0\ ,\ S_{22} = 0\ ,\ S_{23} = 2\beta_1\ ,\ S_{24} = 0 \tag{A.29a-d}$$

Similarly, the BCs at *right* end of the entire C-C beam are given by

$$Y_n(L) = 0\ ,\ Y_n'(L) = 0 \tag{A.30a,b}$$

From Eqs. (12), (15), (16) and (A.30a, b), one obtains

$$V_n(L) = \varphi_n(L)Y_n(L) = 0\ ,\ V_n'(L) = \varphi_n'(L)Y_n(L) + \varphi_n(L)Y_n'(L) = 0 \tag{A.31a,b}$$

Substituting Eq. (14) into Eq. (A.31a, b), one can obtain two equations to take the same forms as Eqs. (A.15a, b) with the coefficients of the constants A_n, B_n, C_n and D_n given by

$$U_{11} = \cos\beta_n L + \cosh\beta_n L\ ,\ U_{12} = \cos\beta_n L - \cosh\beta_n L \tag{A.32a,b}$$

$$U_{13} = \sin\beta_n L + \sinh\beta_n L\ ,\ U_{14} = \sin\beta_n L - \sinh\beta_n L \tag{A.32c,d}$$

$$U_{21} = \beta_n(-\sin\beta_n L + \sinh\beta_n L)\ ,\ U_{22} = \beta_n(-\sin\beta_n L - \sinh\beta_n L) \tag{A.33a,b}$$

$$U_{23} = \beta_n(\cos\beta_n L + \cosh\beta_n L)\ ,\ U_{24} = \beta_n(\cos\beta_n L - \cosh\beta_n L) \tag{A.33c,d}$$

It is noted that, for a beam with the BCs of *left* end to be different from the BCs of *right* end (such as the C-F or C-P beam), the equations regarding its BCs can be obtained from the foregoing equations for the ends with the same BCs.

REFERENCES

Abrate, S. (1995a). Vibration of non-uniform rods and beams. Journal of sound and vibration 185, 703-716.

Auciello, N. M. (1996). Transverse vibrations of a linearly tapered cantilever beam with tip mass of rotary inertia and eccentricity. Journal of sound and vibration 194, 25-34.

Auciello, N. M. and M. J. Maurizi (1997). On the transverse vibrations of tapered beams with attached inertia elements. Journal of sound and vibration 199, 522-530.

Banerjee, J. R. and F. W. Williams (1985). Exact Bernoulli-Euler dynamic stiffness matrix for a range of tapered beams. International journal for numerical methods in engineering 21, 2289-2302.

Bapat, C. N. and C. Bapat (1987). Natural frequencies of a beam with non-classical boundary conditions and concentrated masses. Journal of sound and vibration 112, 177-182.

Carnahan, B., H. A. Luther and J. O. Wilkes (1969). Applied Numerical Methods, John Wiley & Sons, New York.

Cranch, E. T. and A. A. Adler (1956). Bending vibration of variable section beams. Journal of applied mechanics 23, 103-108.

Craver, W. L. and P. Jampala (1993). Transverse vibrations of a linearly tapered cantilever beam with constraining springs. Journal of sound and vibration 166, 521-529.

Lin, H. Y. (2006). On the natural frequencies and mode shapes of a multi-step beam carrying a number of intermediate lumped masses and rotary inertias. Structural engineering and mechanics 22, 701-717.

Lin, H. Y. (2008). Dynamic analysis of a multi-span uniform beam carrying a number of various concentrated elements. Journal of sound and vibration 309, 262-275.

Liu, W. H. and C. C. Huang (1988) Vibrations of a constrained beam carrying a heavy tip body. Journal of sound and vibration 123, 15-29.

Mao, Q. (2011). Free vibration analysis of multiple-stepped beams by using

Adomian decomposition method. Mathematical and computer modeling 54, 756-764.

Meirovitch, L. (1967). Analytical Methods in Vibrations. Macmillan, New York.

Naguleswaran, S. (1992). Vibration of an Euler-Bernoulli beam of constant depth and with linearly varying breadth. Journal of sound and vibration 153, 509-522.

Naguleswaran, S. (2002). Vibration of Euler-Bernoulli beam on elastic end supports and with up to three changes in cross-section. International journal of mechanical sciences 44, 2541-2555.

Rosa, M. A., P. M. Bells and M. J. Maurizi (1995b). Free vibrations of steeped beams with intermediate elastic supports. Journal of sound and vibration 181, 905-910.

Tong, X. and B. Tabarrok (1995c). Vibration analysis of Timoshenko beams with non-homogeneity and varying cross-section. Journal of sound and vibration 186, 821-835.

Torabi, K., H. Afshari and R. M. Heidari (2013). Free vibration analysis of a non-uniform cantilever Timoshenko beam with multiple concentrated masses using DQEM. Engineering solid mechanics 1, 9-20.

Vortex Bladeless (2015). http://vortexbladeless.com/technology.php

Wu, J. S. and H. M. Chou (1999). A new approach for determining the natural frequencies and mode shapes of a uniform beam carrying any number of sprung masses. Journal of sound and vibration 220, 451-468.

Wu, J. S. and M. Hsieh (2000). Free vibration analysis of a non-uniform beam with multiple point masses. Structural engineering and mechanics 9, 449-467.

Wu, J. S. and D. W. Chen (2003). Bending vibrations of wedge beams with any number of point masses, Journal of sound and vibration 262, 1073-1090.

Wu, J. S. and L. K. Chiang (2004). Free vibrations of solid and hollow wedge beams with rectangular and circular cross-sections and carrying any number of point masses. International journal for numerical methods in engineering 60, 695-718.

Wu, J. S. and C. T. Chen (2008). A continuous-mass TMM for free vibration analysis of a non-uniform beam with various boundary conditions and carrying multiple concentrated elements. Journal of sound and vibration 311, 1420-1430.

Wu, J. S. and Y. C. Chen (2011). Out-of-plane free vibration analysis of a horizontally circular curved beam carrying arbitrary sets of concentrated elements. Journal of structural engineering ASCE 137(2), 220-241.